Title

GAMETE MOTION, SEARCH, AND THE EVOLUTION OF ANISOGAMY, OOGAMY, AND CHEMOTAXIS

Authors

Cox, P.A.
Sethian, J.A.

Publication Date

1984-03-01

LBL-17689
Preprint

Lawrence Berkeley Laboratory

UNIVERSITY OF CALIFORNIA

Physics Division

Mathematics Department

To be submitted for publication

GAMETE MOTION, SEARCH, AND THE EVOLUTION OF ANISOGAMY, OOGAMY, AND CHEMOTAXIS

P.A. Cox and J.A. Sethian

March 1984

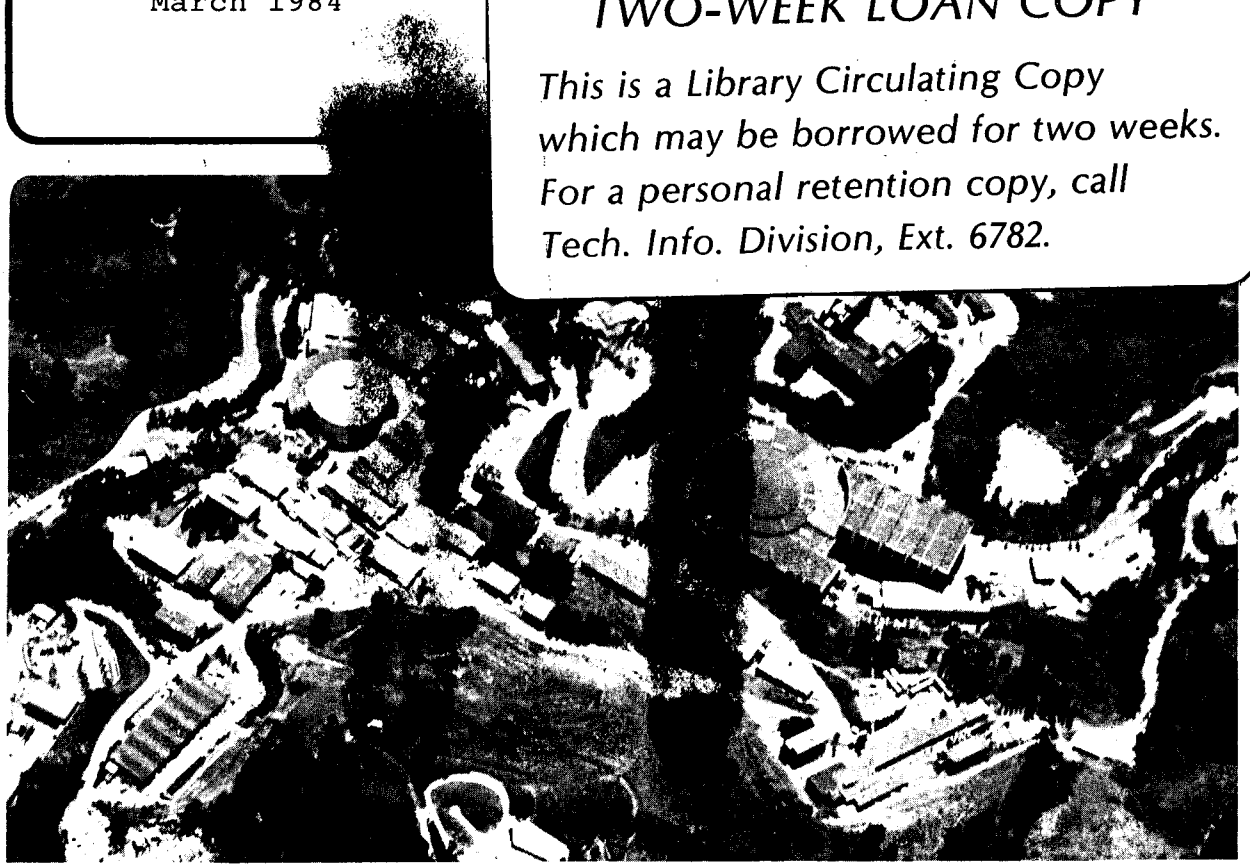

Prepared for the U.S. Department of Energy under Contract DE-AC03-76SF00098

DISCLAIMER

LBL-17689

GAMETE MOTION, SEARCH, AND THE EVOLUTION OF ANISOGAMY, OOGAMY, AND CHEMOTAXIS

Paul Alan Cox*

J.A. Sethian**

*Department of Botany
University of California
Berkeley, California 94720
and
Department of Botany and Range Science
Brigham Young University
Provo, Utah 84602
(present address)

**Department of Mathematics
and
Lawrence Berkeley Laboratory
University of California
Berkeley, California 94720

March 1984

Abstract

We describe mathematical and numerical models to study gamete encounters in two and three dimensions between two different types of gametes. Our results indicate that anisogamy is evolutionarily favored, except for small regions of local stability for isogamy for gametes of small size. The existence of a low adaptive peak for isogamy and a much higher adaptive peak for anisogamy suggests that stochastic forces may be initially important in driving isogamy through the fitness saddle to anisogamy. In addition, we study the related issues of oogamy and chemotaxis and compare computer simulated gamete search patterns to empirical studies of actual chemotactic behaviors.

Numerous ideas have been proposed concerning the potential benefits of sexuality and possible forces favoring the development of separate sexes in higher animals and some plants. However, the evolution of separate male and female gametes that of necessity must have preceeded the evolution of higher forms of sexuality has traditionally received somewhat less attention. Particularly mysterious has been the evolution of separate large female and small male gametes. Within the last decade significant advances have been made in understanding the evolution of anisogamy. Much of this progress springs from the work of Parker, Baker, and Smith (1972) who suggested that the driving force behind the evolution of anisogamy from isogamy is a combination of two factors: many more microgametes than megagametes can be produced from the same mass of gametic material while more fit zygotes will result from the fusion of micro- with megagametes than the fusion of microgametes with microgametes. Bell (1978) extended the results of Parker, Baker, and Smith in analytical form; their results were also expressed in geometric form by Maynard Smith (1978) who used game theory to examine conditions of evolutionary stability for anisogamy. The population genetics of such a mechanism has been explored by Charlseworth (1978), Parker (1978), and Hoekstra (1980). Hoekstra (1982) has also recently analyzed population genetic models for the evolution of mating types in isogamous populations. In a similar vein, Wiese (1982) has suggested that anisogamy could evolve in a monoecious, isogamous taxon if the developmental mechanism that determines the gamete's sex can be genetically dominated by factors determining its size. Paralleling this quantitative approach has been a qualitative exploration of possible energetic advantages of anisogamy. Thus, Ghiselin (1974) has suggested that female gametes specialize in providing zygotes with resources, while male gametes are specialized in searching for female ones. Ghiselin notes that this concept

can be traced to Hertwig (1909) and possibly earlier. In a similar discussion, Williams (1975) suggested that "a primeval conflict between the sexes" resulted from the intense selection for small gametes to overcome the discriminatory mechanisms of the large ones. Parker (1982) has similarly suggested that in externally fertilized species, competition between sperm will maintain anisogamy.

The robustness of the results of Parker, Baker, and Smith (1972) depend, however, on the assumption that the fitness of zygotes increases exponentially with their size -- a assumption that many biologists would find contraintuitive. Thus a mere linear increase in zygote fitness with increasing zygote size will not produce stable anisogamy under the Parker, Baker, and Smith model, as was pointed out by Bell (1978) and the original authors. Although many of the advances in elucidating the evolution of anisogamy spring from the Parker, Baker, and Smith model, several important considerations were ignored in its construction. Of particular importance is the explicit exclusion of the effects of gamete size on rates of encounter: in the Parker, Baker and Smith model, encounter is assumed to be strictly random and not related to size (Parker et al 1971, Parker 1982). At low Reynolds numbers however, from hydrodynamic considerations, it is likely that potential gamete velocity is correlated with gamete size. The effects of differential gamete velocities on encounter rates have not been previously studied, although a comment about encounter rates due to a locomotion based purely on molecular bombardment has recently been made (Schuster and Sigmund 1981). It appears, however, that molecular diffusion as a form of locomotion cannot account for significant probabilities of encounter of gametes of biologically significant sizes, lifespans, and densities.

In the first part of our paper, we describe our investigations into the evolution of anisogamy and oogamy. We derive an analytic expression measuring the number of encounters between gametes as a function of size, given an inverse relationship between gamete size and velocity within a population of a single species, and use this result together with considerations of zygote fitness to explain a mechanism for the evolution of anisogamy and oogamy. To substantiate our conclusions, we then develop a numerical algorithm to simulate gamete-gamete encounters. Using available empirically measured gamete sizes and velocities as input into our algorithm, we perform numerical experiments to analyze encounter rates and invasion fitness. The results of the theoretical and numerical investigations agree well on the mechanism for the stability and instability of isogamy under evolution.

In the second part of our paper, we discuss the role of chemotaxis in the development of optimal searching and encounter strategies between male and female gametes. Chemotaxis increases the probability of an encounter between two gametes by increasing the effective target size and the information available for the search. Thus, rather than relying simply on random motion to produce an encounter between a male and female gamete, the male gamete in some way senses the presence of a released chemotactic substance as an indication of the location of the female. Depending on the sensing and locomotive abilities of the male gamete, a variety of search strategies are possible. We discuss the differences in effectiveness resulting from a few of these potential search patterns and develop a numerical simulation of a particular search strategy in order to examine its effectiveness.

PART ONE: THE EVOLUTION OF ANISOGAMY AND OOGAMY

A. Statement of the Problem

Consider a population of gametes of constant and equal volumes invaded by gametangia capable of producing a variable number of gametes, where the number of gametes produced depends on an equal division of the available gametic mass. The production of gametes through such a division of fixed gametic mass is known to occur in many of the green algae; for example, in the Caulerpales, the genus *Udotea* does not produce differentiated gametangia, the gametes being formed through nuclear division and cytoplasmic cleavage of the protoplasm (Tanner 1981). In the Chlamydomonadinae, division of the vegetative parts through fission into 16, 32, or 64 parts is not uncommon (Fristch 1956). Thus in *Chlamydomonas coccifera* , macrogametes are formed from the ordinary vegetative individual without division while the male gametes are formed by the division of their parent cell into 16 parts and are nearly spherical in shape (Fritsch 1956). We thus imagine a collection of gametes of type A with constant and equal volume V_A invaded by a B gametangium with available reproductive mass V_{MAX} that is divided up into N gametes of type B, each with volume V_B such that $N\,V_B = V_{MAX}$.

We wish to measure the effectiveness of this invasion. Let W_{AB} stand for the fitness of a zygote formed by the fusion between a type A gamete and a type B gamete. Let E_{AB} be the effectiveness of the invasion, defined as

$$E_{AB} = Z_{AB}\ W_{AB} \qquad (1)$$

where Z_{AB} is the number of zygotes formed during the invasion. That is, the success of the invasion is determined by the number of zygotes formed times

the fitness factor assigned to each individual zygote. We may envision the fitness factor W_{AB} as depending in some way on the sizes of the two contributing gametes, that is , $W_{AB} = W_{AB}(V_A, V_B)$. The number of zygotes formed may be written as

$$Z_{AB} = K_{AB}\, R_{AB} \tag{2}$$

where R_{AB} is the number of encounters between type A and B gametes, and K_{AB} is the fraction of encounters that result in fusion. As distinct from previous workers, we suggest that R_{AB} may depend on such factors as the sizes of the two contributing gametes, the model for motion, the initial distribution of gametes and the time allowed. This differs, for example, from the model proposed by Parker et al (1971) and summarized in Parker (1982) in which the encounter rate between the two sets of gametes is constant regardless of their size. As pointed out by the authors themselves, this ignores, among other things, the fact that bigger gametes are easier to hit. The fusion fraction upon contact, K_{AB}, may also be affected by these variables, although species-specific features of reproductive physiology are probably more important. Our invasion effectiveness value E_{AB} may be written as

$$E_{AB} = K_{AB} \cdot R_{AB} \cdot W_{AB} \tag{3}$$

Throughout this paper, we shall assume K_{AB} to be independent of V_A and V_B and therefore without loss of generality assume K_{AB} to be unity; a large and small gamete must fuse if they meet as also must two gametes of equal size.

Our investigations in Part One are based on an examination of Equation (3). Given a collection of type A gametes, volume V_A, what size type B gametes should the invading gametangia produce to maximize the effectiveness of the invasion?

B. Mathematical Investigation

The Model

We consider external fertilization and assume that each gamete has a flagellum capable of producing a constant, given thrust which is the same regardless of the size of the gamete. We idealize both the type A and B gametes as spheres with radii r_A and r_B respectively. At low Reynolds numbers we can use Stokes formula for drag Dr on a sphere moving in a fluid (Landau and Lifshitz 1959) to obtain an inverse relationship between velocity and size, namely that

$$Dr = [6\pi\nu]\, ru \tag{4}$$

where r is the radius of the sphere, u is the velocity, and ν is the fluid viscosity. Thus, in a fixed interval of time under a given thrust T, smaller gametes travel further than larger ones.

There is justification for this model of gamete motion. The Reynolds number is low in such situations (Vogel 1981), and Moestrup (1975) considers spheres to be the "primitive" spermatozoa shape. For the gametes of *Allomyces*, Stokes law can be verified from published data (Pommerville 1978): The small male gametes (radius 5μ) have straight line swimming speed of $100\mu/$ sec, with observed standard deviation of $38\mu/$ sec, while the larger female gametes (radius 10μ) have a swimming speed of $60\mu/$ sec, with observed standard deviation of $8\mu/sec$. This indicates an inverse relationship between size and velocity ($100\times5 \approx 60\times10$) consistent with the Stokes formula as cited above.

Although there are very few quantitative analyses of gamete paths in internally fertilized species, and fewer still for externally fertilized species,

some experimental data is available. For example the motion of uniflagellated male gametes from the aquatic fungus *Allomyces* has been photographed and described (Pommerville 1978) as "short, smooth swimming paths or runs, interrupted by brief periods (a fraction of a second) when the male gametes undergo a spasmodic behavior involving a jerking of the cell body ... followed by a resumption of a smooth swimming pattern, but in a new direction". Similar gamete motility patterns have been observed in internally fertilized mammalian systems. David et al (1981) have found two principal types of trajectory in human spermatozoa; the less frequent type two trajectory is "very irregular due to frequent changes in direction". In cinematic studies of bull spermatozoa, Katz et al (1981) found that " as time progressed, sperm trajectories ... began to become more random in orientation". Katz and Yanagimachi (1980) found observed swimming trajectories to be " convoluted and erratic" in hamster spermatozoa.

In keeping with the above observations, in our model we shall assume that gamete motion consists of smooth, short swimming paths, followed by a sudden reorientation or "jerk" in a new, random direction, after which the swimming motion is resumed. To simplify, we assume that all of the gametes jerk in unison, that is, when one of them jerks, all the rest do also. If one wishes to consider motion in which a moving gamete cannot change directions, this corresponds to assuming that the time between jerks is infinite.

Derivation of Expressions for Encounter Rates and Invasion Effectivness

We assume that the total amount of reproductive mass V_{max} is constant in all gametangia, as in *Chlamydomonas coccifera* (Fritsch 1956), thus we

assume that the mass available to be broken up into type A gametes is the same as that available for type B gametes. Let n_A (n_B) be the number of type A (type B) gametes per unit area, thus, if we assume a mass V_{MAX} of reproductive material per unit area of each type, then

$$n_A = \frac{V_{MAX}}{\frac{4}{3}\pi r_A^3} \qquad n_B = \frac{V_{MAX}}{\frac{4}{3}\pi r_B^3} \tag{5}$$

Let T be the thrust provided by the flagellum, and $u_A(u_B)$ be the corresponding velocity of the type A (B) gamete. From Stokes Law we then have

$$u_A = \frac{T}{r_A} \qquad u_B = \frac{T}{r_B} \tag{6}$$

where we have dropped the factor $6\pi\nu$.

We shall derive an expression for the number of encounters between type A and type B gametes. A collision will occur when the distance between the center of the A gamete and the center of the B gamete is less than r_A+r_B. To make our problem easier, we shall ignore the fact that once a fusion occurs, the pair is no longer available for fertilization and instead concern ourselves in this part with calculating the total number of encounters.

We begin by considering motion in a plane. (After discussing isogamy and anisogamy in two dimensions, we shall consider three dimensional motion). In this section, we shall consider a simpler problem than the one posed by our model of gamete motion, namely that we will evaluate the number of collisions during a time t where t is taken less than the time between jerks, hence during this time each gamete will move in a straight line. The validity of our theoretical results subject to this simplification and the fact that we have neglected removal upon fertilization will have to come from numerical experiments on the original problem. We assume that both A and B gametes are

uniformly distributed, and that the direction each gamete moves is chosen at random. The problem of determining the number of encounters in the above situation is similar to those occurring in the kinetic theory of gases (Smoluchowski 1918, Olander 1929) and search theory (Koopman 1956). Following those investigations, we now calculate the collision rate during a time t.

Given a type B gamete moving with vector velocity $\vec{u}_B$ and a type A gamete moving with vector velocity $\vec{u}_A$, we define the "track angle" φ (see Koopman 1956) between the two as the angle from $\vec{u}_B$ to $\vec{u}_A$ measured in a counterclockwise direction. The vector velocity $\vec{w}$ (See Figure 1a) corresponds to the motion of the A gamete relative to the B gamete. Given speeds u_A and u_B and the track angle φ, we can determine the speed w from the law of cosines, namely

$$w = (u_A^2+u_B^2-2u_Au_B\cos\varphi)^{\frac{1}{2}} \tag{7}$$

We first calculate collisions with reference to a single B gamete, moving with vector velocity $\vec{u}_B$. As stated earlier, we assume a uniform distribution of n_A type A gametes per unit area and that the track angle φ of each A gamete is chosen from a uniform distribution on $[0,2\pi]$; thus the probability that $\varphi_1<\varphi<\varphi_2$ is $(\varphi_2-\varphi_1)/2\pi$. Our technique will be to calculate the number of collisions for a particular track angle φ and then integrate over all possible track angles.

The number of type A gametes per unit area with a particular track angle φ between φ and $\varphi+d\varphi$ is $n_A\frac{d\varphi}{2\pi}$. The speed w of each of these relative to the moving B gamete is given by Equation (7). Since they are moving with vector velocity $\vec{w}$, the only ones that can collide with the B gamete in time t are those located in the striped region in Figure 1b, which corresponds to the cir-

cle of radius r_A+r_B translated in the direction $-\vec{v}$ a distance wt. The area of this region is $2(r_A+r_B)wt$, thus the total number of A gametes of track angle φ that hit the B gamete durin g time t is

$$2(r_A+r_B)wt\, n_A \frac{d\varphi}{2\pi} \tag{8}$$

Integrating over all possible track angles, we find that the total number of collisions R_{A1} between A gametes and the single B gamete is

$$R_{A1} = n_A \frac{2(r_A+r_B)t}{2\pi}\int_0^{2\pi} w d\varphi \tag{9}$$

$$= n_A \frac{(r_A+r_B)t}{\pi}\int_0^{2\pi} (u_A^2+u_B^2-2u_Au_B\cos\varphi)^{\frac{1}{2}} d\varphi$$

$$= n_A \frac{4(r_A+r_B)t}{\pi}(u_A+u_B)\int_0^{\pi/2} (1-\frac{4u_Au_B}{(u_A+u_B)^2}\sin^2\vartheta)^{\frac{1}{2}} d\vartheta$$

Here, we have made the substitution $\vartheta=(\pi-\varphi)/2$. The integral in Equation (9), which we write as $I(u_A,u_B)$, is a complete elliptic integral of the second kind. Since there are n_B type B gametes per unit area, using Equation (5) and Equation (6) and collecting all the constants (including time) into a single constant C we have for the total number of collisions R_{AB} of type A gametes with B gametes per unit area

$$R_{AB} = C\frac{(r_A+r_B)^2}{r_A^4 r_B^4} I(\frac{T}{r_A},\frac{T}{r_B}) \tag{10}$$

The Evolution from Isogamy to Anisogamy

We are now in a position to evaluate a variety of fitness functions and their influence on resulting invasion effectiveness. We can discover some highly suggestive results with the simple assumption that the fitness of the

zygote is the sum of the two contributing volumes, that is,

$$W_{AB} = V_A + V_B$$

This is equivalent to assuming that the fitness of the zygote increases linearly with its size. The invasion effectiveness E thus becomes

$$E_{AB} = C\frac{(r_A+r_B)^2}{r_A^4 r_B^4} I\left(\frac{T}{r_A}, \frac{T}{r_B}\right)\left[\frac{4}{3}\pi(r_A^3+r_B^3)\right] \qquad (11)$$

In order to illustrate different aspects of the function E_{AB} given in Equation 11, in Figure 2 we show a two-dimensional surface plot of E_{AB} with the constant C taken as unity. The unit length scale is the radius of the smallest possible gamete; thus $r_A=2$ denotes a gamete with radius twice that of the minimum sized gamete. In Figure 2a, we let r_A and r_B each range from 1 to 3 and hence consider invasion ranging from small/small ($r_A=r_B=1$) to small/large ($r_A=1, r_B=3$) to large/large ($r_A=r_B=3$). The two axes on the base of the plot, corresponding to r_A and r_B, are increasing in the direction out of the page. The invasion effectiveness E_{AB} is normalized so that the maximum value is one.

We may interpret these results as follows. In Figure 2a, a local maximum in E_{AB} occurs for $r_A=r_B=1$; therefore the invasion is more effective for small, same-sized gametes than it is for small gametes interacting with slightly larger gametes. Note, of course, that the plot is symmetric, since there is no difference accorded to which gamete is called type A and which type B. Thus, we conclude that in this range isogamy is locally stable for small-sized gametes. By this we mean that given a population of type A gametes of unit size, interaction with a smaller number of slightly larger type B gametes will be less profitable than interaction with an equal number of unit sized B gametes. Any perturbation away from isogamy in this regime would lead to a

decrease in overall fitness.

In Figures 2b and 2c, we see that isogamy is in fact not the most effective strategy when we consider wider variations in the sizes between the two types of gametes. In these situations, while the local maximum at $(r_A=1, r_B=1)$ (small/small) persists, E_{AB} increases dramatically along the two sides, corresponding to interaction between big and small gametes. Thus, anisogamy is indicated over these larger ranges. Given a collection of small gametes, it is increasingly more profitable for them to interact with bigger and bigger gametes. Calculation of the minimum of E_{AB} shows that the turnaround point between the tendency towards isogamy and the tendency towards anisogamy occurs for one type of gamete 1.75 times the size of the other. Hence, type B gametes smaller than 1.75 times the radius of type A gametes will not be favored, and the initial isogamy will be maintained. Conversely, type B gametes larger than this critical size will be favored, establishing anisogamy. Note further that if we confine ourselves to only isogamous situations $(r_A=r_B)$, E_{AB} is increasing in the direction pointing towards the point (1,1), indicating that, given equal sized A and B gametes, smaller sizes will always be favored.

Our qualitative conclusions remain the same if one considers instead a fitness function centered around some optimal zygote size. If we let V_{opt} be the optimum size of the zygote, and assume a fitness function corresponding to a bivariate normal distribution with mean at V_{opt} and variance σ^2, then the invasion effectiveness becomes

$$E_{AB} \equiv C\frac{(r_A+r_B)^2}{r_A^4 r_B^4} I\left(\frac{T}{r_A}, \frac{T}{r_B}\right) e^{-\left(\frac{4}{3}\pi(r_A^3+r_B^3)-V_{opt}\right)^2/2\sigma^2} \qquad (12)$$

The value one chooses for the fitness variance σ^2 greatly influences the character of E_{AB}. For example, a very small value of σ^2 would produce a fitness

function that is essentially zero everywhere except for those zygote sizes very near V_{opt} (however, a small local maximum for small isogamous matings will still be present). Conversely, a large value of σ^2 would produce a fitness function close to unity, regardless of gamete size, and thus E would depend solely on the encounter function R_{AB}. In Figure 3a, we plot E_{AB} as given in Equation (12) for radii ranging from 1 to 20 units. We assume an optimum zygote size corresponding to a radius of $(2)^{1/3} \cdot 10$; that is, $V_{opt} = \frac{4}{3}\pi((2)^{1/3} \cdot 10)^3$; and a variance $\sigma^2 = 375$. Obviously, one possible choice would be $r_A = 10, r_B = 10$; one can see however that this is not optimal. Instead, the optimal situation is interaction between gametes of radii approximately 12 and others with radii near 1. As before, anisogamy is indicated everywhere except for a small local adaptive peak of isogamy in the region of small/small encounters. In Figure 3b, we plot E_{AB} for radii ranging from 1 to 5 units, with optimum zygote size corresponding to radius of $(2)^{1/3} \cdot 3$; variance $\sigma^2 = 12.5$. Once again, anisogamy is indicated, with isogamy occupying a local maximum. Here, the transitions are smoother owing to the larger variance (when compared to the range of sizes allowed).

It is now natural to ask, what is the general form of a fitness function for which anisogamy will be favored except for a local maximum for isogamy at small dimensions? We begin by noting that as long as the fitness function W_{AB} depends only on the total zygote volume V formed by fusion between the two gametes, then, for any fixed zygote size, anisogamy produces a larger invasion effectiveness than isogamy. To see that this is so, given zygote size V, we consider all combinations r_A, r_B such that $(r_A^3 + r_B^3) = V$, where we have ignored the factor $\frac{4}{3}\pi$. We solve for r_A and use Equation (10) to get

$$E_{AB} = \frac{\left\{(V-r_B^3)^{1/3} + r_B\right\}^2}{(V-r_B^3)^{4/3} r_B^4} I\left(\frac{T}{(V-r_B^3)^{1/3}}, \frac{T}{r_B}\right) W_{AB}(V) \qquad (13)$$

where now, W_{AB} is the same for all pairs r_A, r_B and hence can be ignored. One can check that, for fixed V, the minimum of E_{AB} occurs when $r_B = (V/2)^{1/3}$ in which case $r_B = r_A$.

We now examine the effect on E_{AB} of increasing r_B with r_A held fixed at 1. We have

$$E_{AB}(1,r_B) = \frac{(1+r_B)^2}{r_B^4} I\left(T, \frac{T}{r_B}\right) W_{AB}(r_B)$$

Zygote fitness is crucial in the evaluation of the split between isogamy and anisogamy. Consider a fitness function of the form r_B^p. Then

$$E_{AB}(1,r_B) = \left\{\frac{1}{r_B^{4-p}} + \frac{2}{r_B^{3-p}} + \frac{1}{r_B^{2-p}}\right\} I\left(T, \frac{T}{r_B}\right)$$

For $p<2$, this is a decreasing function and thus isogamy is always indicated and interaction between small type A and small type B gametes produces the largest value of E. Conversely, for $p>2$, anisogamy is indicated, since then, for large values of r_B, E_{AB} is an increasing function. In particular, a linear function of *volume* will favor anisogamy in all but the smallest ranges. This result is in contrast to the Parker, Baker and Smith (1971) model that suggests anisogamy to be stable if and only if zygote fitness increases exponentially with zygote size. The presence of local isogamy for small dimensions is due to the fact that the encounter rate drops very rapidly as r_B increases. Unless the fitness function can overcome this at small values of r_B, a local isogamy maximum will be indicated.

Higher Dimensions/Alternative Models

Suppose we now consider motion in three dimensions. Given a single type B gamete moving with vector velocity $\vec{u}_B$, we again assume a uniform distribution of n_A type A gametes, where now n_A is the number per unit *volume*. We assume that each A gamete has an equal chance of going in any direction. The track angle φ is not uniformly distributed on $[0,\pi]$ (See Figure 1c); the probability of a track angle φ between φ_1 and φ_2 is the area of the strip between φ_1 and φ_2 on a sphere of radius R, divided by the total surface area of that sphere. The area of the strip is $\int_{\varphi_1}^{\varphi_2} 2\pi(R\sin\varphi)R\,d\varphi$ and the total surface area of the sphere is $4\pi R^2$, hence the probability of a track angle between φ and $\varphi+d\varphi$ is $\frac{1}{2}\sin\varphi\,d\varphi$. The speed w of each A gamete is once again given by Equation (7) and only those in the *sphere* of radius (r_A+r_B) translated up in the direction $-\vec{w}$ a distance wt can hit the B gamete. Integrating over all possible track angles, we find that the total number of collisions R_{A1} between A gametes and the single B gamete is

$$R_{A1} = \frac{n_A\pi(r_A+r_B)^2t}{2}\int_0^{\pi}(u_A^2+u_B^2-2u_Au_B\cos\varphi)^{\frac{1}{2}}\sin\varphi\,d\varphi \qquad (14)$$

$$= \frac{n_A\pi(r_A+r_B)^2t}{6}\frac{1}{u_Au_B}\left[(u_A^2+u_B^2+2u_Au_B)^{\frac{3}{2}} - (u_A^2+u_B^2-2u_Au_B)^{\frac{3}{2}}\right]$$

Collecting all the constants (including time) into a single constant C and using Equations (5) and (6), we have for the total number of collisions R_{AB} of type A gametes with B gametes per unit volume

$$R_{AB} = C\frac{(r_A+r_B)^2}{r_A^2r_B^2}\left[\left|\frac{1}{r_A}+\frac{1}{r_B}\right|^3-\left|\frac{1}{r_A}-\frac{1}{r_B}\right|^3\right] \qquad (15)$$

Using the collision factor R_{AB} for encounters in three dimensions given by Equation (15), we analyzed invasion effectiveness for various fitness functions as was done in the two dimensional case. Our qualitative results remain unchanged; anisogamy is favored except for a small fitness peak of locally stable isogamy for small-sized gametes. One must be careful comparing the collision rate in two dimensions (Equation (10)) with the rate in three dimensions (Equation (15)), since in the former we speak of unit area whereas in the latter of unit volume. We can make the following comparison. Suppose we have a single type B gamete and a given number of type A gametes. If we put the B gamete at the center of a square of side length l and uniformly distribute the A gametes over that square, more of them will hit the B gamete than if we distribute the same number of A gametes uniformly over a cube of side length l centered around the B gamete.

As mentioned earlier, our mathematical analysis is for a simpler problem than our original model of gamete motion, namely that we have assumed that each gamete moves in a straight line for a time t. As an alternative, at the other extreme we can assume that each gamete changes direction infinitely often. This view of gamete motion is similar to Brownian motion (Einstein 1926), in which particles suspended in a fluid move in an irregular manner due to bombardment by molecular motion. Although the locomotion of each gamete is due to a flagellum providing a thrust, rather than momentum imparted by colliding molecules, Stokes law for the drag on a sphere can be applied in both cases and we still have an inverse relation between speed and radius. Imagine a collection of $n_A(n_B)$ type A (B) particles of radius r_A (r_B) per unit volume, all undergoing Brownian motion. One can compute the number of collisions per unit time by direct calculation (Smoluchoswki 1918, Olander 1929) or by making use of the fact that the random motion of a large

particle due to molecular bombardment can be regarded as a diffusion, in which the concentration of the substance being diffused is represented by the probability of finding the particle in any particular place (Einstein 1926, Landau 1959, Moelwyn-Hughes 1961). In three dimensions, the collision rate R_{AB} is of the form

$$R_{AB} = C\frac{(r_A+r_B)^2}{r_A r_B} n_A n_B \qquad (16)$$

The constant C depends, in the Brownian motion case, on the Boltzman constant, the temperature and the viscosity. In our interpretation, C would be proportional to the strength of the thrust provided by the flagellum; the bigger the thrust, the higher the encounter rate. Using the collision factor in Equation (16) and our expressions for n_A and n_B, we analyzed invasion effectiveness for various fitness functions. Once again, our qualitative results remain unchanged; anisogamy is favored except for a small fitness peak of locally stable isogamy for small-sized gametes. Even if one ignores locomotion by a flagellum and simply considers gamete motion due to Brownian motion, the inverse relation between speed and size produces the same situation of favored anisogamy vs. local isogamy at small ranges (a comment about encounter rates in the case of gamete motion due solely to molecular bombardments was made in Shuster and Sigmund 1981).

Another point to be mentioned in the context of this discussion is dimension. As stated earlier, for our first model the collision rate in two dimensions is higher than in three dimensions; for the diffusion path model, it is not difficult to show that random walks in a plane are recurrent, while in three dimensions they are not [see Sethian 1976; Cox 1983]. By this, we mean that two particles undergoing random walks in two dimensions become arbitrarily close with probability one; however, this does not hold in three dimensions.

The above can be seen as an explanation why some gametes move to the surface before executing their search: their encounter probabilities are increased (Cox 1983). For example, in the acroporiid and some faviid coral species, gametes are extruded as bouyant egg-sperm bundles that rise to the surface and then break apart (Harrison et al 1984). A botanical example of such surface-seeking behavior can be seen in the gametes of sea-lettuce *Ulva lactuca*. The gametophyte is heterothallic and during reproduction the vegetative cells give rise to isogamous gametes along the thallus margins. This division occurs at night with gametes being shed early in the morning (Carter 1926). In total darkness *Ulva* gametes swim random paths, but when illuminated with a blue-violet light, they swim rapidly towards the source at speeds up to 300 μm per second, or over 2000 times their body length per minute (Haxo and Clendenning 1953). It is of interest that the spectra of light necessary to trigger positive phototaxis is different from that necessary for their photosynthesis (Haxo and Clendenning, 1953); this difference possibly allows them to orient themselves and swim to the surface even from deep water. After the gametes fuse, there is a reversal of the light response, with the resultant zygotes becoming negatively phototactic. This likely aids the zygote in finding and attaching to the substrate. Eyespots and other phototactic systems appear to be widespread in some green algae taxa, being an important step in their early evolution (Melkonian 1982), Such phototactic devices may help in this manner to increase mating efficiencies as well as serving to maintain the position of the organisms in photosynthetically advantageous areas. Eyespots are generally lacking, however, in gametes of the more advanced green algae (Moestrup 1975) but are very frequent in the brown algae. In some brown algae, however, phototaxis is not always positive. Thus the anisogametes of the brown alga *Colpomenia* (Scytosiphonaceae) are

negatively phototactic. In this taxon, however, fertilization still takes place in two dimensions rather than three, since it occurs at the substrate surface, with male gametes swarming around the female gametes after settling (Clayton 1979).

The Evolution from Anisogamy to Oogamy

Given the tendency towards anisogamy, we now briefly discuss the development of oogamy, which appears to be an advanced condition in algae (Moestrup 1975). From Stokes law, the larger the gamete, the slower the velocity and the shorter the resultant distance it travels in a unit time for equal thrust. Consequently, for large gametes, the flagellum has little effect, and motion is limited. As a result, the invasion effectiveness between small and large gametes does not change significantly if we remove the flagellum from the larger gametes. Thus the flagellum may prove to be very ineffective in propelling a macrogamete and is unlikely to be maintained through evolution. Not only does the presence of a flagellum serve little in increasing search efficiencies for a very large gamete, it may also be counterproductive from the point of view of the evolution of chemotaxis. Given that an female releases chemotactic substances as information about its location for neighboring male gametes, it is obviously ill-advised for the female to move during or after doing so. We therefore suggest that selection for oogamy in an anisogamous taxon will be accelerated once the macrogamete exceeds a certain size range and chemotaxis is evolved. We shall return to these issues in the section on numerical simulation and in Part Two where we discuss chemotactic search strategies.

C. Numerical Modelling of Invasion Effectiveness

In this section, we describe a series of numerical experiments designed to test the validity of our theoretical results. We begin with a description of our algorithm for gamete motion and fertilization. Due to limited computer resources, we confine ourselves to the algorithm applied to two dimensional motion; the gametes, however, will be represented as spheres.

At each time $t=n\Delta t$, $n=0,1,2,3...$, $\Delta t=$ time step, we let $n_A(t)$ be the number of type A gametes, where the position of the i^{th} one is given by (xa_i^n, ya_i^n). Similarly, let (xb_i^n, yb_i^n) be the position of the i^{th}, $0\le i\le n_B(t)$ type B gamete at time $n\Delta t$.

Given an initial distribution of type A and B gametes (that is, the values $(xa_i^0, ya_i^0), i=1,n_A(0)$, $(xb_i^0 yb_i^0), i=1,n_B(0)$), we advance the position of both types of gametes by moving the gamete in a random direction with speed u drawn from a Gaussian distribution with mean inversely proportional to the radius and variance prescribed. That is,

$$xa_i^{n+1} = xa_i^n + (u_A \cos\varphi_A)\,\Delta t$$

$$ya_i^{n+1} = ya_i^n + (u_A \sin\varphi_A)\,\Delta t$$

and

$$xb_i^{n+1} = xb_i^n + (u_B \cos\varphi_B)\,\Delta t$$

$$yb_i^{n+1} = yb_i^n + (u_B \cos\varphi_B)\,\Delta t$$

where φ_A and φ_B are angles chosen randomly from a uniform distribution on $(0,2\pi)$, u_A is drawn from a normal distribution with mean C/r_A and appropriate variance, and similarly u_B is drawn from a random distribution with mean C/r_B, where C is a constant. This is in keeping with our Stokes law

assumption for the drag on a sphere; the bigger particles move slower.

In order to determine those pairs of type A and type B gametes that have fertilized, we must determine if they collide during the time step. This is done as follows. Assume that at the beginning of a time $n\Delta t$ a particular type A gamete is at (xa^n, ya^n) and a particular type B gamete is at (xb^n, yb^n). Let (xa^{n+1}, ya^{n+1}), (xb^{n+1}, yb^{n+1}) be their positions at time $(n+1)\Delta t$. We express the distance between the two gametes as a function of time and compute the minimum distance during the time step. The distance squared $d(\alpha)$ can be written as

$$d(\alpha) = \left\{\left\{\alpha(xa^{n+1})+(1-\alpha)(xa^n)\right\} - \left\{\alpha(xb^{n+1})+(1-\alpha)(xb^n)\right\}\right\}^2$$
$$+ \left\{\left\{\alpha(ya^{n+1})+(1-\alpha)(ya^n)\right\} - \left\{\alpha(yb^{n+1})+(1-\alpha)(yb^n)\right\}\right\}^2$$

where $0 \leq \alpha \leq 1$. Since this function is a quadratic in α, its minimum can easily be found analytically; if the minimum distance is less than r_A+r_B and occurs for a value of α between 0 and 1, then the two gametes have collided. This is counted as a successful encounter (fusion) and the pair is removed from the calculation.

In our first experiment, we studied the invasion of a large population of small gametes by gametes of varying sizes. To identify the components in this discussion, we refer to the small gametes as type A gametes, and the larger gametes as type B. As a basis for our simulation, we have used data derived in a series of elegant cinematographic experiments on human spermatozoa by Dresdner and Katz (1981) who measured a male gamete head radius of 1.25μm, and a swimming speed of 43μm per second, at a concentration of 10^8 gametes/ml. Such measurements apply to internal fertilization situations; we have felt free to employ them in our model, however we have assumed a

density of gametes per unit length an order of magnitude less than the above for our external fertilization model. Placing the type A gametes on a uniform square grid a unit distance apart, this corresponds to type A gamete radius of .0013 units; we allow each one to travel an average distance of .052 units per unit time step.

Into this population at $t=0$, we inject in the center of the domain a type B gametangium, with reproductive mass $M = \frac{4}{3}\pi(.052)^3$, capable of producing N type B gametes of equal volume V_B such that $NV_B = M$. Thus, if $N=1$, the gametangia forms a single type B gamete with radius 40 times larger than the incipient type A gametes, and for $N>1$, the radius of type B gametes is correspondingly smaller. Here, the speed of the type B gamete is inversely proportional to its radius, as explained earlier (the constant is determined from the type A gametes, namely $C=(.0013)\times(.052)$).

Whenever a type B gamete "collides" with a type A gamete, we regard this as a successful fusion and remove the type B gamete from the population. To cut down on computer time, a 10 by 10 grid (100) of type A gametes was used; upon fusion with a type B gamete, the A gamete is returned to its initial position and allowed to move about once again. This cuts down on the number of elements in the calculation without altering the general character of the solution.

In Table 1, we show the results of this calculation. Experiments were performed using N type B gametes, with N ranging from 1 to 1000 (Column 1), corresponding to B gametes with radius 40 to 4 times as large as the A gamete radius. In Column 2, the radii of the type A and B gametes are given. In each experiment, the calculation was stopped after the gametes had taken 1800 random steps; this "lifespan" or window of fertilization competency was

chosen so that over 5% of type B gametes had been fertilized in the final (N=1000) experiment. For each value of N, 500 different trials were performed; the mean number of collisions is given in Column 3. In Column 4, the invasion effectiveness is given, calculated by computing the zygote fitness (here, taken as the volume of the total fused zygote formed) times the mean number of collisions. In those trials where all the type B gametes were fertilized before the lifespan ended, the calculation was stopped and the next trial begun.

As can be seen from the table, our numerical simulation agrees well with the theoretical model. As the radius of the type B gametes increases, although N decreases, the invasion effectiveness increases, showing the tendency towards anisogamy as predicted. On the other hand, we note that when the radius of the type B gametes becomes very small, the effectiveness increases as size decreases indicating local isogamy, as also predicted. Extensive calculations showed that the minimum effectiveness occurred for N around 475. This corresponded to a type B gamete size of radius about 5 times bigger than the type A gamete; this is in good agreement with our theoretically calculated estimate. (We stress that our theoretical model did not remove fused pairs from the calculation).

In Table 2, we repeat the above experiment, assuming a shorter lifespan and stopped the calculation after half as many steps. Again, we see the increased effectiveness associated with encounter between small and large gametes; note that the values for E are much lower since there is less time allowed for collisions (we shall explain what we mean by this point below). A local effectiveness maximum for small dimensions is still present in the ranges considered, however the size of this peak is much smaller than that of the

longer lifespan case. This indicates that although in small/small interactions there are a larger number of participants, the shortened lifespan and resulting decrease in the number of collisions lowers the effectiveness in this regime. This indicates that if isogamy exists, it should be among not only small sized gametes, but ones that live a long time or have a very wide window of availability for fertilization, as contrasted to taxa whose gametes rapidly lose fertilization competency as they age (Pommerville 1982).

In Tables 3 and 4 we reverse the previous two experiments, considering now a population of large gametes (r_A=.052) invaded by decreasing sized gametes. Once again, we see the advantages of anisogamy, in which the most effective strategy is encounters between small gametes and large ones. The presence of the large number of zero effectiveness levels for large sized type B gametes is due to the fact that if both of the types of gametes are large, they move very slowly and thus have a small chance of colliding during a short gametic lifespan. Thus, in the even shorter lifespan case, a large number of small gametes is required before any measurable interaction takes place.

We turn next to the issue of oogamy. In Tables 5 and 6 (Lifespan 1800 and 900, respectively), we let a population of small gametes interact with decreasing sized gametes in which the flagellum are removed, hence these gametes stay fixed. For small values of N, that is, few and large gametes, the value of E is comparable with those in Tables 1 and 2 respectively, indicating that these gametes are large enough and few enough to be fertilized without the need for a lot of movement. However, for large numbers of N, (many type B gametes), there is no mechanism to carry the B gametes away from the injection site, hence during the allotted lifespan not enough type A gametes make it to the injection site. For these large values of N, E is very small; note that the local

pocket of isogamy is no longer present. In these regimes, the flagellum is of critical importance in carrying the B gametes away from the injection site.

Finally, we consider the issue of lifespan. As mentioned earlier, the shorter the fertilization window (the time during which both A and B gametes are active), the more pronounced the benefits of anisogamy. Since each type B gamete requires its own A gamete for fusion, injection of the type B gametangia at a point into a collection of small A gametes means that once neighboring A gametes have been fused, more time is required for new A gametes to come into the domain and fuse with the remaining B gametes. Hence, given a short fertilization window, one would want to use relatively few B gametes so that all of them could be fertilized by close neighboring A gametes.

With this in mind, we may thus use our numerical model for gamete motion to provide a very rough estimate of the fertilization window for human sperm and egg, based on the experimentally measured data (Katz 1980) used in the previous calculations: sperm head radius r_A of 1.25 μm and a swimming speed of 43 μm/sec. The radius of the human egg is about 20-30 μm and thus the egg radius is about 20 times larger than the sperm radius.

We now make the following assumption. *Assume that the invasion effectiveness E associated with this measured ratio (20 to 1) of egg to sperm radius is optimal.* By this, we mean that during a fertilization window time T, invasion by an even smaller number of larger type B gametes for the same time T provides little change in the invasion effectiveness E. We may thus calculate T by examining the invasion effectiveness as a function of lifetime for different values of N, the number of divisions of the type B gametangium.

We numerically modelled the injection of flagellated type B gametes into a collection of flagellated type A gametes, where, as before, we assumed that

the type B reproductive mass could be broken up into N equally sized B gametes. N=1 corresponded to a single type B gamete with radius 40 times larger than the A gamete radius; N=8 corresponded to eight B gametes each with radius 20 times larger than the A gametes, etc. Thus, N=8 yielded a type B gamete size comparable to that of the human egg. We calculated the invasion effectiveness E as a function of lifespan; by this we mean that at every time step we computed the total number of successful fusions times the fitness factor. For each value of N, 50 trials were conducted and the results were averaged. Each trial was stopped when all the type B gametes had been fertilized.

In the the above experiment, given N type B gametes, if one waits long enough, all of them will be eventually fertilized. Conversely, given a very short fertilization window, only for small values of N will all the B gametes be fertilized. In Figure 4, we plot the invasion effectiveness against the allowed interaction time for various values of N. Here, the invasion effectiveness E is normalized to be unity when all the type B gametes are fertilized, and the time axis is in units of 100 seconds. We performed the experiment for N=1, 8, 16, 32, 64, 128, and 512.

Under our assumption that the invasion effectiveness associated with N=8 (egg radius twenty times that of sperm) for the lifespan T is optimal, we can use Figure 3 to obtain a rough estimate of the value of T. For small values of T, say around 4000 secs, the value of E for N=1 is much higher (and in fact, is unity) than the value for N=8, indicating that, given a lifespan of length 40, invasion with N=1 is more profitable than with N=8, hence there is a drive towards fewer than 8 type B gametes. For large values of T, say around 15000 secs, the value of E for both N=32 and for N=8 are unity, indicating that

there is no selective force to push from 32 divisions of the gametangium to 8 divisions. Reversing the argument, since we know that the human egg radius is about 20 times larger than that of the male gamete, we can see from Figure 3 that a fertilization window of $T=10000$ secs or about three hours would roughly correspond to the situation in which fewer divisions are no more profitable, and more divisions are less effective. This figure is in the range of fertilization window estimates used in *in vitro* fertilization studies which show fertilization competency of human eggs to decay rapidly after 7- 12 hours (R. Urie, personal comm.). Of course, we must point out that we have ignored a multitude of factors in egg/sperm fertilization and have grossly oversimplified the situation, however the results obtained are quite suggestive.

PART TWO: THE EVOLUTION OF CHEMOTAXIS

A. The Role of Chemotaxis

In Part One we have discussed the evolution of anisogamy and oogamy from isogamy. Although anisogamy increases the net product of encounter rates and zygote fitness, the probability of successful fertilization of a female gamete could be increased even further if it had the ability to broadcast information concerning its location to nearby male gametes. By the same token, any male gamete that is able to successfully interpret this chemotactic signal and modify its search patterns accordingly will have a high probability of successfully fertilizing a female gamete. Thus the potential benefit of a chemotactic system is that the effective female target size is increased and the

search pattern of the male changed accordingly.

While the concentration of chemotatic substances produced by the female is a continuous function of the distance from the point of release, it is likely that the male gamete senses mainly two discrete regions. At a large distance from the female, any chemotatic substances present are at such low concentrations that they are undetectable by the male gamete. Closer to the female, however, we can imagine a chemotatic aura whose boundary represents the minimum threshold concentration of chemotactic substance detectable by the male gamete. Given this situation, we can then ask what type of search patterns on the part of the male gamete will both reduce the search time and increase the probability of locating and fertilizing the female. In addressing this question, it is convenient to consider these two chemotactic domains separately.

In the outer region which is devoid of information about the female gamete location, a good strategy would be one which increases the probability of bumping into the boundary of the chemotactic aura. We can thus imagine a strategy in which the male gamete covers a significant amount of territory, searching on a scale that would locate the presence of the chemotactic boundary, rather than on a finer scale that would locate an object the size of the female gamete.

In the inner region where the male gamete senses the chemotattractant, one strategy would be for the male to always proceed in the direction of the maximum concentration gradient until reaching the female. Such a plan, however, requires highly sophisticated gamete behavior in two ways: the male gamete must be able to both sense the concentration gradient and continuously steer accordingly. Between such advanced strategies and those based on

purely random motion can lie a variety of search patterns with varying degrees of effectiveness. For example in the brown alga *Ectocarpus siliculosus* male gametes drastically alter their swimming behavior in the presence of the chemotactic substance ectocarpen by changing their "normal straightforward locomotion to tight circles in the vicinity of an attractant source" (Muller 1976). These male gametes surround the female in a vigorous circular movement (Hartmann 1934, Muller 1981).

B. Analysis of a Particular Chemotactic System

Perhaps the most detailed observations of the effect of chemotaxis on gamete motility have been provided by Pommerville (1978), who studied the fungus *Allomyces* and photographed the swimming patterns of male gametes in the presence and absence of chemotactic substances. The male swims in an arc a short distance, followed by a sudden jerk or reorientation, after which the swimming motion is resumed, but now in a new direction. (Pommerville 1978, Figure 5a). Female gametes produce the chemoattractant sirenin which alters the motion of the male gamete. In the presence of sirenin, the male gametes adopt a "long spiral path that extends towards the sirenin source". These paths do not have the numerous jerks observed in motion without sirenin; " ... once moving away from the female cells, the male gamete stops swimming, undergoes one or two jerks that reorient the cells to the sirenin gradient and swims again in another smooth run" (Pommerville 1978, Figure 5b). The change in direction produced by the jerk is always of the same magnitude, however it changes from left to right under the influence of sirenin. Pommerville also identifies a third region, very close to the sirenin source, in which the

male gamete jerks much more rapidly, initiating "many quick changes of direction".

Thus, the search pattern of the male gamete has two different modes: a polygonal path outside the chemotactic aura where the movement is characterized by arc swim followed by jerk/reorientation followed by arc swim, and a smooth spiral path inside the chemotactic aura interrupted by jerks only when moving away from the sirenin source. What is of particular interest in this search strategy is that there are only two fundamental components: the arc swim and the jerk. Given these two basic components, the parameters that influence the actual path taken are the length of the arc l, the reorientation jerk angle ϑ and the arc angle φ, where φ is the angle that subtends the given arc (See Figure 6).

In order to analyze how the characteristics of this search strategy depend on the values of φ, ϑ and l, we developed a numerical simulation of the above gamete motion. We imagine a female gamete at the origin of a coordinate system and assumed a steady-state radially decreasing concentration profile of chemoattractant around the female gamete. We assumed that the high concentration area of sirenin exists inside a circle of radius r_1 centered at the origin which we call Region 1. Motion inside this area is characterized by the increased number of jerks and hence shorter swimming paths. Proceeding outwards, the next level, Region 2, which is characterized by the spiral swimming paths, occupies the annulus with inner radius r_1 and outer radius r_2. Finally, outside the circle of radius r_2 in Region 3 we assume that sirenin cannot be detected by the male gamete and thus movement is characterized by the arc swim/jerk/arc swim motion.

As input parameters, we must supply mean values and standard deviations for the arc length l, the arc angle φ and the reorientation jerk angle ϑ. For the sake of discussion, we assume that the starting point for the male gamete lies in Region 3, placing it in the non-sirenin region. Given a starting position and initial direction ω_i, we choose an arc length l^* from a normal distribution with mean l and the appropriate standard deviation and an arc angle φ^* from a normal distribution with mean φ and appropriate standard deviation. From this, we construct the appropriate arc, that is, the one of length l^* with initial tangent in the direction ω_i and subtended angle φ^*. At the end of the arc, the tangent points in a new direction ω_f; a jerk angle ϑ^* is then chosen from the appropriate normal distribution and ω_f is changed by ϑ^*, producing a new initial direction ω_i for the next arc.

When the gamete moves into Region 2 (determined by computing the distance between its position and the origin) the motion changes accordingly. As noted before, in this region, jerks only occur when the male is moving away from the female gamete. (We note that this motion is highly reminiscent of those described in "bang-bang" control theory, see Bellman (1967)). We model this as follows: the distance from the male gamete to the female is compared before and after the arc is traversed. If the male gamete is determined to have moved closer, (moved up the concentration gradient), no jerk occurs (ϑ^* is taken as 0) and the next arc is constructed; conversely, if the male moves away, a jerk angle is chosen (with opposite sign than in Region 3) and a new direction obtained in the usual manner. Finally, when the gamete moves into Region 1, where the concentration is high and motion is characterized by rapid jerks and short swimming paths, we return to the arc swim/jerk/arc swim pattern. However, we now chose jerks much more often, resulting in shorter paths. We arbitrarily chose these jerks to occur five times more often

than they do in Region 3.

In Figures 5c and 5d we show the results of two numerical experiments using this algorithm. Using the data from Pommerville (1978) as input, we take a mean path length between jerks as 50μm (standard deviation 17μm) and a mean jerk angle as 60° (S.D. 17°). From the published photographs, we measured the arc angle φ to be approximately 45°; we assumed a zero variance in this value. The female was placed at (0,0), and the field of vision is 1200μm. The values for r_1 and r_2 were chosen arbitrarily; we assumed a combined female plus male radius of 7.5μm, an inner radius r_1=50μm and and outer radius r_2=350μm; the regions are labelled 1, 2 and 3. In Figure 5c, the male gamete started at the point (350.,350.) (labelled S) in a direction 240° counterclockwise from the positive x axis. In Figure 5d, the male gamete started at (400.,0) in the positive x direction.

As can be seen from the figures, our numerical scheme compares favorably with the photographed male gamete tracks. In Region 3, where the sirenin goes undetected, the arc swim/jerk/arc swim pattern creates the polygonal path that searches for the edge of the chemotactic aura. If the length l and jerk reorientation angle ϑ were always constant, the path would be a polygon with curved sides (and in fact, with the given parameters, a hexagon), thus the variations in l and ϑ are responsible for the motion away from the starting point. Whether or not the gamete finds the edge of the boundary of Region 2 is, of course, a function of where it starts and how long it searches. If the gamete reaches Region 2, it goes into the spiral mode in which jerks are allowed only when moving away from the source. One can see that our simple algorithm creates the spiral structure in the photographs, and in fact demonstrates the way in which this spiral "bends in" towards Region 1. Inside Region

1, the rapid jerking motion creates a sort of random motion that eventually carries the male gamete into contact with the female; Figure 5c depicts a male gamete that found the female much faster than the one in Figure 5d.

Our numerical simulation thus shows that the entire search strategy consists of two motions: the arc swim and the reorientation jerk. We now ask, what determines the choices for l, φ and ϑ?

In answering this question, we shall concentrate on examining only the effect of different choices for the arc angle φ on search efficiency in Regions 1 and 2. In order to limit our study to these two regions, we take $r_2=\infty$, thus motion consists solely of the spiral path and the rapid jerks. With l normally distributed with mean 50μm and ϑ normally distributed with mean 60°, we varied the arc angle φ from 1° (essentially a straight line segment) to 90° (tight spirals). Our experiment proceeded as follows: For each angle φ, we started a male gamete at the point (300,0) in an initial trial direction ω and calculated the length of the path taken between the start and fertilization. We performed 360 such trials for each arc angle φ, varying the initial direction ω one degree at a time between 1° and 359°; after all the trials were performed for a particular value of φ, a mean path length was computed.

The results of this experiment are given in Table 7, comparing the arc angle to the mean path length. The minimum path occurs for an arc angle around 44°, certainly well within the tolerance of our measurements of the arc angle from the photographs. This result remained essentially unchanged when we repeated the experiment with the male gamete starting at a distance 450μm and 600μm, We conclude that an arc angle near 45° minimizes that path length between tight spirals ($\varphi \gg 45°$) that proceed slowly towards the female and larger arcs ($\varphi \ll 45°$) which reach the neighborhood of the female

fairly quickly but have a difficult time finally locating it. Starting the male gamete closer than 250μm produced higher optimal arc angles, suggesting a lower bound for the radius of the chemotactic boundary surrounding Region 2 of at least 250μm; the actual radius is known to be significantly greater (Pommerville private comm.) It is possible that starting the male gamete much further out will produce a lower optimal angle, thus suggesting an upper bound for the chemotactic boundary; such experiments, however, were beyond our resources and were not performed. The effectiveness of the measured values for l and v also awaits further study.

DISCUSSION

We have shown through both analytical and computer models that anisogamy produces the largest values of invasion effectiveness everywhere except for a region of local stability for isogamy at small gamete sizes. We can thus imagine a fitness surface (Fig. 2c.) characterized by a very high fitness peak corresponding to anisogamy and a much smaller fitness peak corresponding to isogamy connected by a shallow fitness saddle. In this sense the fitness topography for gamete size (Figs. 2 and 3) corresponds to the notion of adaptive topography conceived by Sewall Wright (1927, 1977) with the gene frequencies of isogamous gametes being under control of the low isogamous adaptive peak. As Wright stated: "Very rarely, the crossing of a shallow saddle may bring the set of gene frequencies under control of a peak several orders of magnitude higher than previously and lead to a rapid advance" (Wright 1977, p.450). We suggest that the evolution of anisogamy from isogamy represents just such a "rapid advance" as primitive taxa moved through the shallow fitness saddle

from the small fitness hill of isogamy to the fitness Everest of anisogamy. Possible events that could have propelled isogamous taxa across this fitness saddle might include unique environmental changes, extensive random drift, other random processes, and other unique events that "have no variance and as such cannot be represented by a stochastic distribution" (Wright 1977). We would thus predict isogamy to characterize relatively "primitive" taxa with small gametes and, as a result, small zygote sizes. This prediction is in accordance with the results of Madison and Waller (1983) who examined 130 species of algae in 17 different orders and found a strong correlation between small zygote size and isogamy. Although we have not been successful in our search of the literature in locating a data set that compares the sizes of isogamous gametes to anisogamous gametes for a large number of taxa , the experience of both phycologists and mycologists suggests that isogametes are usually significantly smaller than anisogametes (J, West, P. Silva, J. Taylor, S. Rushforth, personal comm.). We would welcome attempts by other investigators to test this in a systematic fashion. Our numerical simulations also suggest the existence of strong selection for wide windows of fertilization in isogamous taxa, but systematic data with which to test this prediction are similarly lacking.

It is clear, however, that the evolutionary transition from isogamy to anisogamy to oogamy (and the evolution of chemotaxis at any one of these stages) is the result of a complex adaptive topography generated in part by hydrodynamic factors that can be examined analytically as well as numerically. The existence of multiple fitness peaks in this adaptive topography suggests that arguments for anisogamy need to be tempered by examination of regions of local stability for alternative reproductive strategies.

We have also analyzed, using a numerical simulation, the chemotactic search patterns of *Allomyces* and have found that just two motility behaviors can be combined with appropriate sensory apparatus to generate a highly sophisticated search pattern. We discuss possible benefits of chemotactic systems for other taxa.

SUMMARY

Using mathematical models and numerical simulations, we propose a new model for the evolution of anisogamy from isogamy. We suggest that the relative sizes of the two types of gametes directly affect encounter probabilities and if fertilization occurs, the fitness of the resultant zygote. We propose that the product of encounter probability and zygote fitness can be maximized by gametes of greatly different size. However, regions of local stability for isogamy at small gamete sizes are indicated by both our analytical results and our numerical simulations. We thus postulate a complex adaptive topography for the evolution of anisogamy with a fitness saddle separating the low adaptive peak of isogamy and the higher adaptive peak for anisogamy. Our model also allows us to make rough estimates of the length of fertilization window for gametes given empirical data concerning their sizes and swimming speeds. As a result, we predict the gametes of isogamous taxa to generally have a longer period of fertilization competency than gametes of anisogamous taxa.

Using considerations of gamete motion, we predict decreasing benefit of flagella to female gametes as the female gamete size increases, thus providing impetus for the evolution of oogamy in taxa with large female gametes. Using computer simulations we also analyze factors favoring the evolution of

chemotaxis and compare simulated gamete search patterns to empirical studies of actual chemotactic behaviors.

ACKNOWLEDGEMENTS

Our collaboration was facilitated through the Danforth Foundation Fellowship Program. We thank H. Baker, I.Baker. B. Cox, M. Donaghue, A. Fogelson, E. Guerrant, W. Graves, O. Hald, J. Pommerville, S. Rushforth, P. Silva, J. Maynard Smith, J. Taylor, and J. West for comments and facilities. We thank also J. Pommerville and *Experimental Cell Research* for permission to publish photographs of *Allomyces* gamete search patterns. We are grateful to the Lawrence Berkeley Laboratory and the University of California for computer time. During this study Cox was supported by a Miller Fellowship by the Miller Institute for Basic Research in Science and Sethian was supported by a National Science Foundation Mathematical Sciences Post-doctoral Fellowship. This work was supported in part by the Director, Office of Energy Research, Office of Basic Energy Sciences, Engineering, Mathematical and Geosciences Division of the U.S. Department of Energy under contract DE-AC03-76SF00098.

LITERATURE CITED

Bell, G.J. 1978. The evolution of anisogamy. J. theor. Biol 73: 247-270

Bellman, R. 1967. Introduction to the mathematical theory of control processes. Academic Press, New York.

Charlesworth, B. 1978. The population genetics of anisogamy. J. theor. Biol. 73: 347-359

Cox, P. A. 1983. Search theory, random motion, and the convergent evolution of pollen and spore morphology in aquatic plants. Am. Nat. 121:9-31.

Clayton, M. N. 1979. The life history and sexual reproduction of *Colpomenia peregrina* (Scytosiphonaceae, Phaeophyta) in Australia. Br. phycol. J. 14: 1-10.

David, G., S. Serres, and P. Jouannet. 1981. Kinematics of human spermatozoa. Gamete Research 4: 83-95.

Dresdner, R.D. and Katz, D.F. 1981. Relationships of mammalian sperm motility and morphology to hydrodynamic aspects of cell function. Biol. of Reprod. 25: 920-930.

Einstein, A. 1926. Investigations on the theory of the Brownian movement. Methuen, London.

Fritsch, F. E. 1956. The structure and reproduction of the Algae. Cambridge Univ. Press, Cambridge.

Ghiselin, M. T. 1974. The economy of nature and the evolution of sex. Univ. of California Press, Berkeley.

Harrison, P.L., Babcock, R.C., Bull, G.D., Oliver, J.K., Wallace, C.C., and Willis, B.L. 1984. Mass spawning in tropical reef corals. Science 223: 1186-1188.

Hartmann, M. 1934. Untersuchungen uber die Sexualitat von *Ectocarpus siliculosus*. *Arch. Protistenk. 83: 110-153.*

Haxo, F. T. and K. A. Clendenning. 1953. Photosynthesis and phototaxis in *Ulva*

lactuca gametes. Biological Bulletin 105: 103-114.

Hertwig, O. 1909. The cell: outlines of general anatomy and physiology. Swan Sonnenschein, London.

Hoekstra, R.F. 1982. On the asymmetry of sex: evolution of mating types in isogamous populations. J. theor. Biol. 98: 427-451.

Hoekstra, R.F. 1980. Why do organisms produce gametes of only two different sizes? Some theoretical aspects of the evolution of anisogamy. J. theor. Biol. 87: 785-793.

Katz, D.F. and R. Yanagimachi. 1980. Movement characteristics of hamster spermatozoa within the oviduct. Biol. Reproduction 22: 759-764.

Koopman, B.O. 1956. The Theory of Search, Part I. Kinematic Bases. Operations Research, 4: 324-346.

Landau, L. D. and E. M. Lifshitz. 1959 Fluid mechanics. Pergamon Press, Oxford.

Madsen, J. D. and D. M. Waller. 1983. A note on the evolution of gamete dimorphism in algae. Am. Nat. 121: 443-447.

Maynard Smith, J. 1978. The evolution of sex. Cambridge Univ. Press ,Cambridge.

Melkonian, M. 1982. Structural and evolutionary aspects of the flagellar apparatus in green algae and land plants. Taxon 31: 255-265.

Moelwyn-Hughes, E. A. 1961. Physical chemistry, 2nd ed. Pergamon Press, Oxford.

Moestrup, O. 1975. Some aspects of sexual reproduction in eucaryotic algae. *pages* 23-35 *in* Duckett, J. G. and P. A. Racey, eds., The biology of the male gamete. Supplement No. 1 to the Biol. J. Linn. Soc, 7.

Muller, D.G. 1981. Sexuality and sex attraction. *pages* 661-674 *in* Lobban, C.S. and M.J. Wynne, eds, The biology of seaweeds. University of California Press, Berkeley.

Muller, D.G. 1976. Quantitative evaluation of sexual chemotaxis in two marine brown algae. Z. Pflanzenphysiol. 80: 120-130.

Olander, A. 1929. Studien uber Brombernsteinsaure III. 10. Einige theretische Betrachtungen uber bimolekulare Reaktionen in verdunnten Losungen. Zeitschrift f. physik. Chemie.144: 118-133.

Parker, G. A. 1982. Why are there so many tiny sperm? Sperm competition and the maintenance of two sexes. J. theor. Biol. 96: 281-294.

Parker, G. A. 1978. Selection on non-random fusion of gametes during the evolution of anisogamy. J. theor. Biol. 73: 1-28.

Parker, G.A., Baker, R.R. and V.G.F. Smith. 1971. The origin of gamete dimorphism and the male-female phenomenon. J. theor. Biol. 36: 529-553.

Pommerville, J. 1978. Analysis of gamete and zygote motility in *Allomyces*. Experimental Cell Research 113: 161-172.

Present, R. D. 1958. Kinetic theory of gases. Mcgraw-Hill, New York.

Schuster, P. and K. Sigmund. 1981. A note on the evolution of sexual dimorphism. J. theor. Biol. 94: 107-110.

Sethian, J. A. 1976. Brownian motion and potential theory. Undergraduate Thesis, Princeton University.

Tanner, C. E. 1981. Chlorophyta: life histories. *pages* 218-247 *in* Lobban, C.S. and M.J. Wynne, eds, The biology of seaweeds. University of California Press, Berkeley.

Smoluchowski, M. 1918. Versuch einer mathematischen Theorie der Koagulationskinetik kolloider Losungen. Zeitschrift f. physik. Chemie 17: 129-168.

Vogel, S. 1981. Life in moving fluids. Willard Grant Press, Boston.

Wiese, L. 1981. On the evolution of anisogamy from isogamous monoecy and on the origin of sex. J.. theor. Biol. 89: 573-580.

Williams, G. C. 1975 . Sex and evolution. Princeton Univ. Press, Princeton.

Wright, S. 1977. Evolution of the genetics of populations. Vol. 3. Experimental results and evolutionary deductions. The University of Chicago Press, Chicago.

Wright, S. 1929. Evolution in a Mendelian population. Anat. Record 44: 287

TABLE 1 : Invasion of small gametes (r_A=.0013) by decreasing-sized flagellate gametes ($r_B = \frac{(.052)}{N^{1/3}}$): Lifespan=1800 Steps

N	r_B / r_A	MEAN COLLISIONS	EFFECTIVENESS E
1	.0520/.0013	0.93	0.5489×10^{-3}
2	.0413/.0013	1.65	0.4859×10^{-3}
3	.0366/.0013	2.15	0.4236×10^{-3}
4	.0328/.0013	2.46	0.3634×10^{-3}
5	.0304/.0013	2.81	0.3315×10^{-3}
6	.0286/.0013	2.84	0.2793×10^{-3}
7	.0272/.0013	3.25	0.2734×10^{-3}
8	.0260/.0013	3.19	0.2348×10^{-3}
9	.0250/.0013	3.33	0.2180×10^{-3}
10	.0241/.0013	3.49	0.2055×10^{-3}
17	.0202/.0013	3.95	0.1371×10^{-3}
25	.0178/.0013	4.48	0.1057×10^{-3}
37	.0156/.0013	4.90	0.7817×10^{-4}
50	.0142/.0013	5.85	0.6898×10^{-4}
62	.0131/.0013	5.98	0.5693×10^{-4}
75	.0123/.0013	6.26	0.4921×10^{-4}
87	.0117/.0013	6.85	0.4650×10^{-4}
100	.0112/.0013	6.72	0.3964×10^{-4}
150	.0097/.0013	8.43	0.3317×10^{-4}
200	.0089/.0013	10.06	0.2973×10^{-4}
300	.0078/.0013	12.62	0.2490×10^{-4}
400	.0071/.0013	15.86	0.2350×10^{-4}
450	.0069/.0013	17.76	0.2340×10^{-4}
500	.0066/.0013	20.62	0.2447×10^{-4}
575	.0063/.0013	23.32	0.2410×10^{-4}
650	.0060/.0013	26.74	0.2447×10^{-4}
725	.0058/.0013	31.64	0.2599×10^{-4}
800	.0056/.0013	33.25	0.2478×10^{-4}
900	.0053/.0013	42.32	0.2808×10^{-4}
1000	.0052/.0013	58.62	0.3188×10^{-4}

TABLE 2 : Invasion of small gametes (τ_A=.0013) by decreasing-sized flagellate gametes ($\tau_B = \frac{(.052)}{N^{1/3}}$): Lifespan=900 Steps

N	τ_B / τ_A	MEAN COLLISIONS	EFFECTIVENESS E
1	.0520/.0013	0.73	0.4299×10^{-3}
2	.0413/.0013	1.13	0.3345×10^{-3}
3	.0366/.0013	1.32	0.2599×10^{-3}
4	.0328/.0013	1.45	0.2140×10^{-3}
5	.0304/.0013	1.50	0.1773×10^{-3}
6	.0286/.0013	1.51	0.1484×10^{-3}
7	.0272/.0013	1.73	0.1460×10^{-3}
8	.0260/.0013	1.54	0.1138×10^{-3}
9	.0250/.0013	1.67	0.1098×10^{-3}
10	.0241/.0013	1.82	0.1071×10^{-3}
17	.0202/.0013	1.96	0.6818×10^{-4}
25	.0179/.0013	2.25	0.5300×10^{-4}
37	.0156/.0013	2.40	0.3823×10^{-4}
50	.0142/.0013	2.73	0.3220×10^{-4}
62	.0131/.0013	2.75	0.2618×10^{-4}
75	.0123/.0013	2.95	0.2322×10^{-4}
100	.0112/.0013	3.13	0.1843×10^{-4}
150	.0097/.0013	3.88	0.1523×10^{-4}
200	.0089/.0013	4.35	0.1281×10^{-4}
300	.0078/.0013	5.51	0.1082×10^{-4}
400	.0071/.0013	6.32	0.9305×10^{-5}
450	.0068/.0013	6.88	0.9004×10^{-5}
500	.0066/.0013	7.61	0.8970×10^{-5}
575	.0063/.0013	8.12	0.8317×10^{-5}
650	.0060/.0013	8.90	0.8064×10^{-5}
800	.0056/.0013	10.22	0.7530×10^{-5}
900	.0053/.0013	13.18	0.8625×10^{-5}
1000	.0052/.0013	14.13	0.8324×10^{-5}

TABLE 3 : Invasion of big gametes (r_A=.052) by decreasing-sized flagellate gametes ($r_B = \frac{(.052)}{N^{1/3}}$): Lifespan=1800 Steps

N	r_B / r_A	MEAN COLLISIONS	EFFECTIVENESS E
1	.0520/.052	0.00	0.0000
2	.0413/.052	0.00	0.0000
3	.0366/.052	0.00	0.0000
4	.0328/.052	0.00	0.0000
5	.0304/.052	0.00	0.0000
6	.0286/.052	0.00	0.0000
7	.0272/.052	0.00	0.0000
8	.0260/.052	0.00	0.0000
9	.0250/.052	0.00	0.0000
10	.0241/.052	0.00	0.0000
17	.0202/.052	0.00	0.0000
25	.0179/.052	0.00	0.0000
37	.0156/.052	0.002	0.1209×10^{-5}
50	.0142/.052	0.006	0.3604×10^{-5}
67	.0131/.052	0.014	0.8368×10^{-5}
75	.0123/.052	0.020	0.1193×10^{-4}
87	.0117/.052	0.070	0.4170×10^{-4}
150	.0097/.052	0.62	0.3676×10^{-3}
200	.0089/.052	1.77	0.1050×10^{-2}
300	.0078/.052	6.46	0.3820×10^{-2}
400	.0071/.052	16.11	0.9515×10^{-2}
500	.0066/.052	28.78	0.1698×10^{-1}
650	.0060/.052	54.04	0.3187×10^{-1}
725	.0058/.052	70.92	0.4182×10^{-1}
800	.0056/.052	88.40	0.5213×10^{-1}
900	.0053/.052	112.42	0.6628×10^{-1}
1000	.0052/.052	143.95	0.8486×10^{-1}

TABLE 4 : Invasion of big gametes (r_A=.052) by decreasing-sized flagellate gametes ($r_B = \frac{(.052)}{N^{1/3}}$): Lifespan=900 Steps

N	r_B / r_A	MEAN COLLISIONS	EFFECTIVENESS E
1	.0520/.052	0.00	0.0000
2	.0413/.052	0.00	0.0000
3	.0366/.052	0.00	0.0000
4	.0328/.052	0.00	0.0000
5	.0304/.052	0.00	0.0000
6	.0286/.052	0.00	0.0000
7	.0272/.052	0.00	0.0000
8	.0260/.052	0.00	0.0000
9	.0250/.052	0.00	0.0000
10	.0241/.052	0.00	0.0000
17	.0202/.052	0.00	0.0000
25	.0179/.052	0.00	0.0000
37	.0156/.052	0.00	0.0000
50	.0142/.052	0.00	0.0000
67	.0131/.052	0.00	0.0000
75	.0123/.052	0.00	0.0000
87	.0117/.052	0.00	0.0000
150	.0097/.052	0.00	0.0000
200	.0089/.052	0.00	0.0000
300	.0078/.052	0.00	0.0000
400	.0071/.052	1.41	0.8325×10^{-3}
500	.0066/.052	3.25	0.1921×10^{-2}
650	.0060/.052	7.89	0.4654×10^{-2}
725	.0058/.052	10.23	0.4182×10^{-2}
800	.0056/.052	15.05	0.5213×10^{-2}
900	.0053/.052	21.65	0.1276×10^{-1}
1000	.0052/.052	30.74	0.1812×10^{-1}

TABLE 5 : Invasion of small gametes (r_A=.0013) by decreasing-sized unflagellate gametes ($r_B = \frac{(.052)}{N^{1/3}}$): Lifespan=1800 Steps

N	r_B / r_A	MEAN COLLISIONS	EFFECTIVENESS E
1	.0520/.0013	0.92	0.5454×10^{-3}
2	.0413/.0013	1.62	0.4770×10^{-3}
3	.0366/.0013	1.89	0.3726×10^{-3}
4	.0328/.0013	2.10	0.3101×10^{-3}
5	.0304/.0013	2.13	0.2518×10^{-3}
6	.0286/.0013	1.99	0.1953×10^{-3}
7	.0272/.0013	1.81	0.1523×10^{-3}
8	.0260/.0013	1.77	0.1307×10^{-3}
9	.0250/.0013	1.74	0.1140×10^{-3}
10	.0241/.0013	1.70	0.1004×10^{-3}
17	.0202/.0013	1.58	0.5503×10^{-4}
25	.0178/.0013	1.47	0.3473×10^{-4}
37	.0156/.0013	1.38	0.2207×10^{-4}
50	.0142/.0013	1.32	0.1558×10^{-4}
67	.0131/.0013	1.25	0.1101×10^{-4}
75	.0123/.0013	1.22	0.9607×10^{-5}
87	.0117/.0013	1.18	0.8053×10^{-5}
100	.0112/.0013	1.24	0.7314×10^{-5}
150	.0097/.0013	1.13	0.4467×10^{-5}
200	.0089/.0013	1.04	0.3087×10^{-5}
300	.0078/.0013	0.99	0.1962×10^{-5}
400	.0071/.0013	0.98	0.1452×10^{-5}
450	.0068/.0013	0.88	0.1166×10^{-5}
500	.0066/.0013	0.83	0.9877×10^{-6}
575	.0063/.0013	0.80	0.8305×10^{-6}
650	.0060/.0013	0.86	0.7871×10^{-6}
725	.0058/.0013	0.85	0.7028×10^{-6}
800	.0056/.0013	0.89	0.6634×10^{-6}
900	.0053/.0013	0.81	0.5375×10^{-6}
1000	.0052/.0013	0.80	0.4785×10^{-6}

TABLE 6 : Invasion of small gametes (τ_A=.0013) by decreasing-sized unflagellate gametes ($\tau_B = \frac{(.052)}{N^{1/3}}$): Lifespan=900 Steps

N	τ_B / τ_A	MEAN COLLISIONS	EFFECTIVENESS E
1	.0520/.0013	0.75	0.4452×10^{-3}
2	.0413/.0013	1.09	0.3233×10^{-3}
3	.0366/.0013	1.15	0.2269×10^{-3}
4	.0328/.0013	1.06	0.1569×10^{-3}
5	.0304/.0013	1.13	0.1333×10^{-3}
6	.0286/.0013	1.06	0.1040×10^{-3}
7	.0272/.0013	0.94	0.7959×10^{-4}
8	.0260/.0013	0.93	0.6846×10^{-4}
9	.0250/.0013	0.91	0.5994×10^{-4}
10	.0241/.0013	0.90	0.5312×10^{-4}
17	.0202/.0013	0.83	0.2896×10^{-4}
25	.0178/.0013	0.79	0.1861×10^{-4}
37	.0156/.0013	0.73	0.1171×10^{-4}
50	.0142/.0013	0.69	0.8198×10^{-5}
67	.0131/.0013	0.66	0.5819×10^{-5}
75	.0123/.0013	0.64	0.5073×10^{-5}
87	.0117/.0013	0.62	0.4237×10^{-5}
100	.0112/.0013	0.57	0.3357×10^{-5}
150	.0097/.0013	0.53	0.2081×10^{-5}
200	.0089/.0013	0.50	0.1487×10^{-5}
300	.0078/.0013	0.55	0.1060×10^{-5}
400	.0071/.0013	0.44	0.8638×10^{-6}
450	.0068/.0013	0.41	0.5366×10^{-6}
500	.0066/.0013	0.41	0.4855×10^{-6}
575	.0063/.0013	0.44	0.4572×10^{-6}
650	.0060/.0013	0.38	0.3443×10^{-6}
725	.0058/.0013	0.39	0.3229×10^{-6}
800	.0056/.0013	0.43	0.3165×10^{-6}
900	.0053/.0013	0.37	0.2421×10^{-6}
1000	.0052/.0013	0.36	0.2120×10^{-6}

TABLE 7 : Average search path length for male gamete as a function of arc angle φ (360 trials per angle) in a chemotactic system.

φ (degrees)	Mean Path (μm)	φ (degrees)	Mean Path (μm)
1	89701	46	2131
2	87222	47	2093
3	82580	48	2115
4	76199	49	2125
5	69867	50	2164
6	63184	51	2226
7	54731	52	2250
8	47348	53	2231
9	45041	54	2297
10	35442	55	2281
11	27760	56	2342
12	26764	57	2383
13	22789	58	2331
14	16229	59	2399
15	13759	60	2495
16	13247	61	2467
17	11605	62	2516
18	9551	63	2605
19	7651	64	2588
20	7168	65	2623
21	5948	66	2733
22	5890	67	2715
23	4477	68	2800
24	4872	69	2769
25	4148	70	2666
26	3830	71	2760
27	3739	72	2763
28	3345	73	2781
29	3261	74	2852
30	2913	75	2825
31	2755	76	2836
32	2622	77	2852
33	2561	78	2918
34	2354	79	2934
35	2297	80	2946
36	2365	81	2963
37	2130	82	3012
38	2165	83	3024
39	2230	84	3035
40	2132	85	3064
41	2065	86	3058
42	2139	87	3002
43	2030	88	3007
44	2011	89	2971
45	2032	90	2957

LEGENDS TO FIGURES

1. a. Definition of track angle φ and relative velocity vector $\vec{w}$ in two dimensions. $\vec{u}_A$ is the vector velocity of the A gamete and $\vec{u}_B$ is the vector velocity of the B gamete.

b. Set of A gametes that can hit B in time t.

c. Definition of track angle φ and relative velocity vector $\vec{w}$ in three dimensions. $\vec{u}_A$ is the vector velocity of the A gamete and $\vec{u}_B$ is the vector velocity of the B gamete.

2.

a. The adaptive topography of invasion effectiveness for gametangia producing gamete sizes ranging between one and three times the radius of the smallest gamete in the population. The shaded diagonal in this and all subsequent diagrams indicates isogamous matings. Note that within this size range, isogamy has the highest adaptive peak for anisogamy.

b. The adaptive topography of invasion effectiveness for gamete sizes ranging between one and seven times the radius of the smallest gamete in the population. In this size range, the adaptive peaks for anisogamy and isogamy are roughly of equal height.

c. The adaptive topography of invasion effectiveness for gamete size ranging between one and twenty time the radius of the smallest gamete in the popula-

tion. Note that in this larger size range, anisogamy is indicated with isogamy representing a region of local stability.

3.

a. The adaptive topography of invasion effectiveness assuming a fitness function of the form $e^{-[((r_A^3+r_B^3)-2000)/750]^2}$.

b. The adaptive topography of invasion effectiveness assuming a fitness function of the form $e^{-[((r_A^3+r_B^3)-54)/25]^2}$.

4.

Normalized invasion effectiveness plotted against lifespan measured in units of 100 seconds.

a: $N=1$

b: $N=8$

c: $N=16$

d: $N=32$

e: $N=64$

f: $N=512$

g: $N=128$.

5.

a. Photograph of male gamete motion of the fungus *Allomyces* in the absence of sirenin (Pommerville 1978).

b. Photograph of male gamete motion of the fungus *Allomyces* under the influence of sirenin

c. Numerical simulation of male gamete motion, initial position S.

d. Numerical simulation of male gamete motion, initial position S.

6. Definitions in Region 3 of jerk angle ϑ, arc angle φ and arc length l for motion of male in fungus *Allomyces*

FIGURE 1

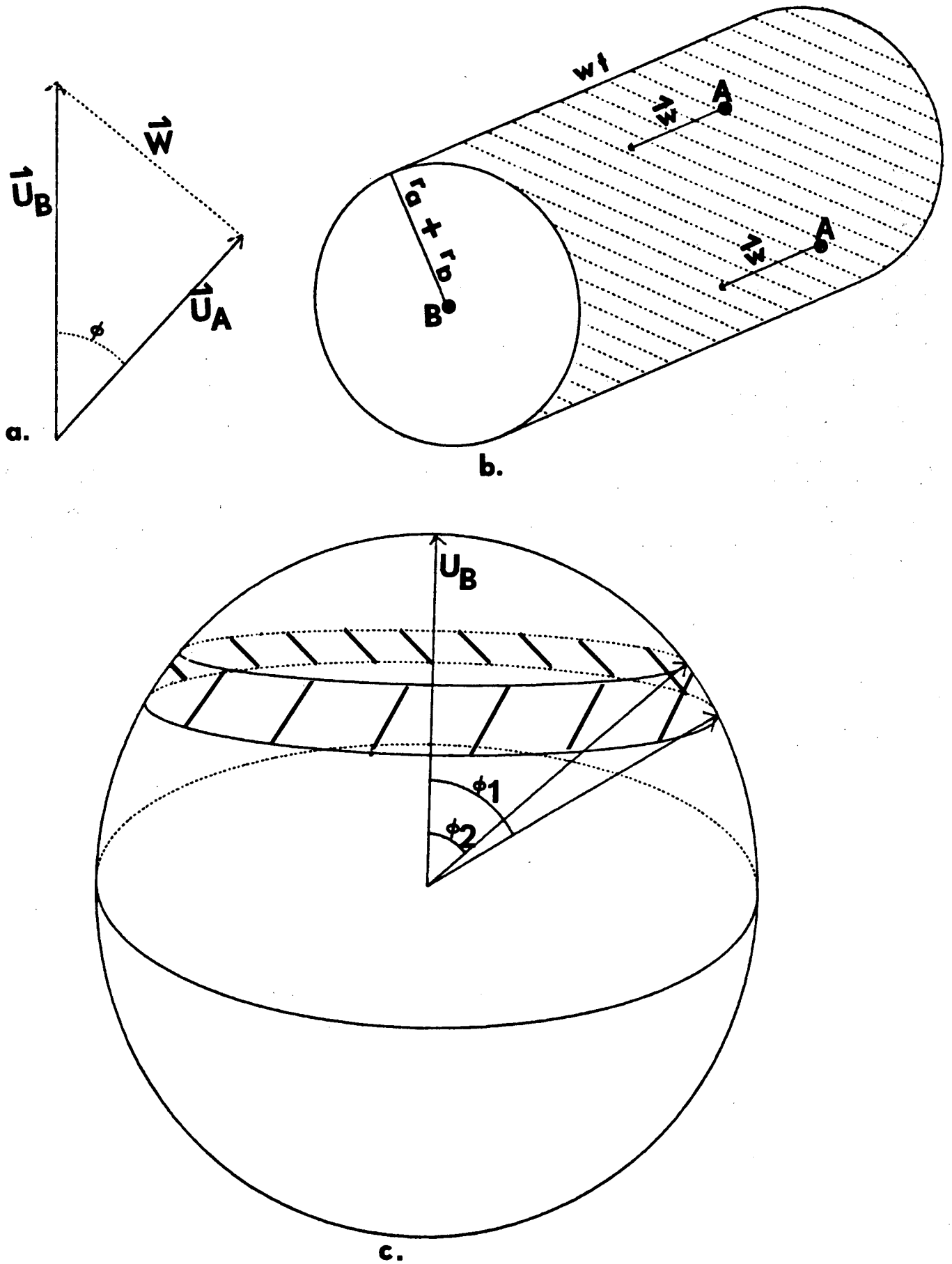

FIGURE 2

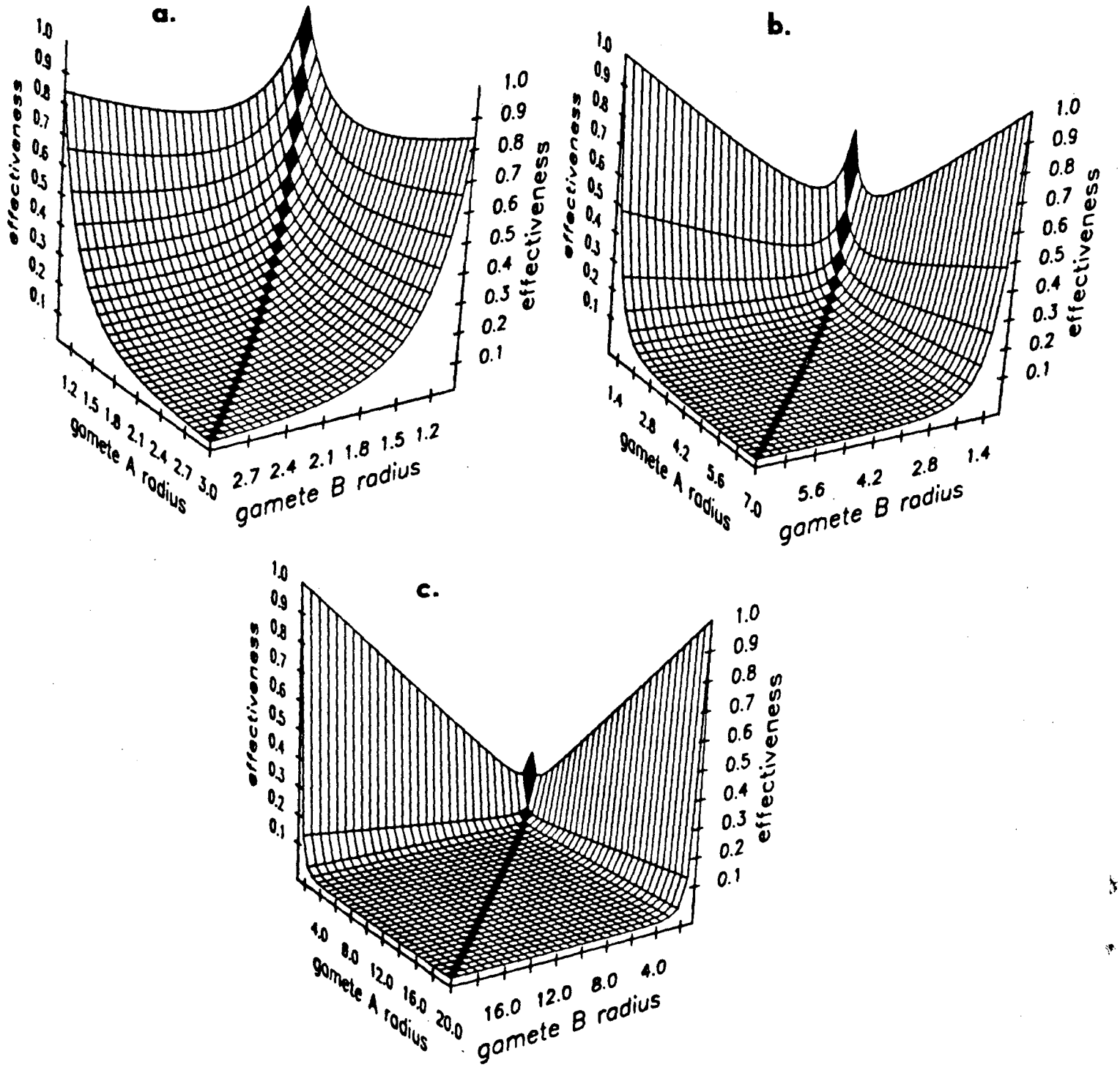
a.
effectiveness
1.0 0.9 0.8 0.7 0.6 0.5 0.4 0.3 0.2 0.1
1.2 1.5 1.8 2.1 2.4 2.7 3.0
gamete A radius
2.7 2.4 2.1 1.8 1.5 1.2
gamete B radius
b.
effectiveness
1.4 2.8 4.2 5.6 7.0
gamete A radius
5.6 4.2 2.8 1.4
gamete B radius
c.
effectiveness
4.0 8.0 12.0 16.0 20.0
gamete A radius
16.0 12.0 8.0 4.0
gamete B radius

FIGURE 3

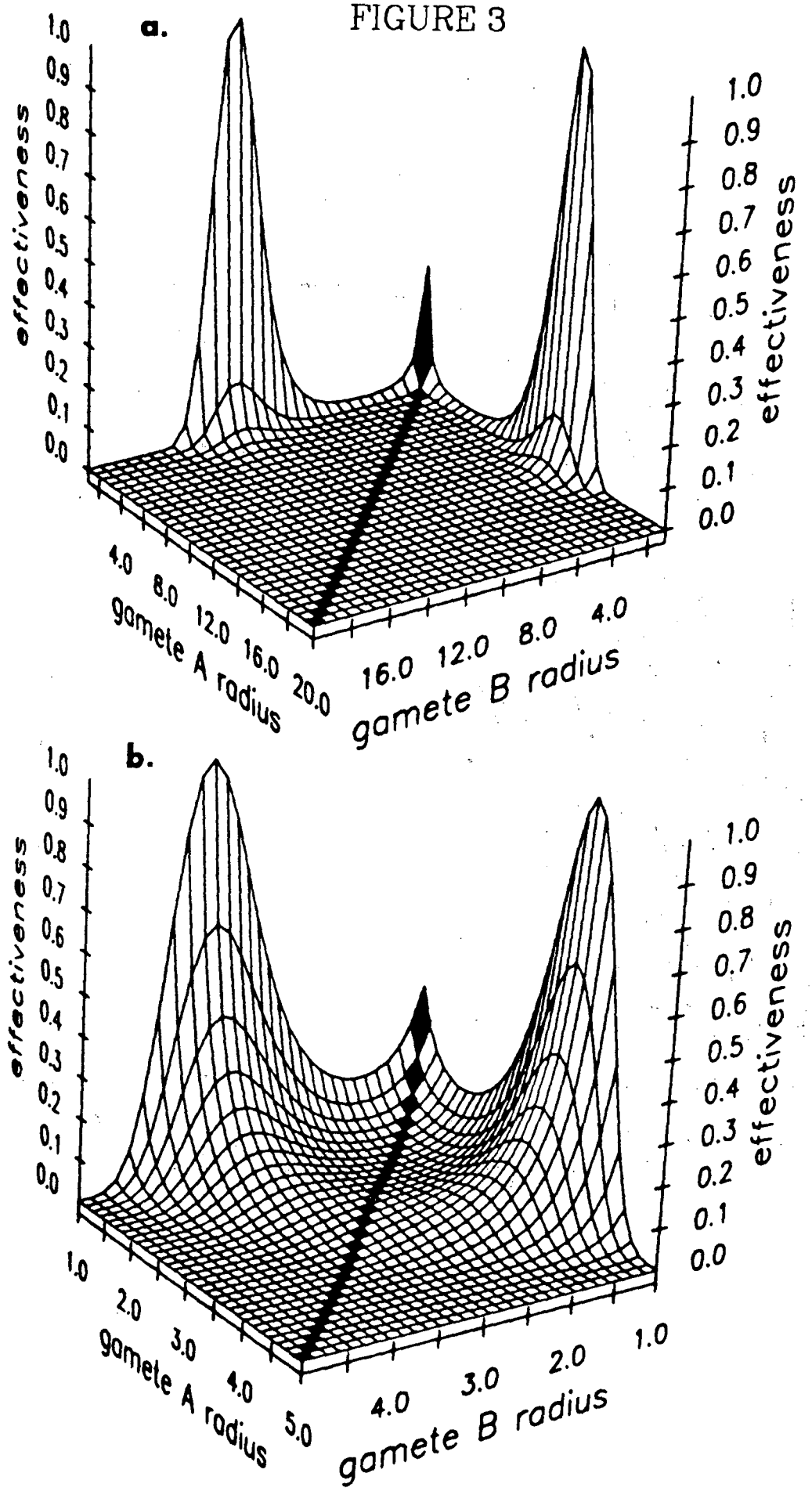
a.
effectiveness
1.0
0.9
0.8
0.7
0.6
0.5
0.4
0.3
0.2
0.1
0.0
4.0
8.0
12.0
16.0
20.0
gamete A radius
16.0
12.0
8.0
4.0
gamete B radius
effectiveness
b.
effectiveness
1.0
2.0
3.0
4.0
5.0
gamete A radius
4.0
3.0
2.0
1.0
gamete B radius
effectiveness

FIGURE 4

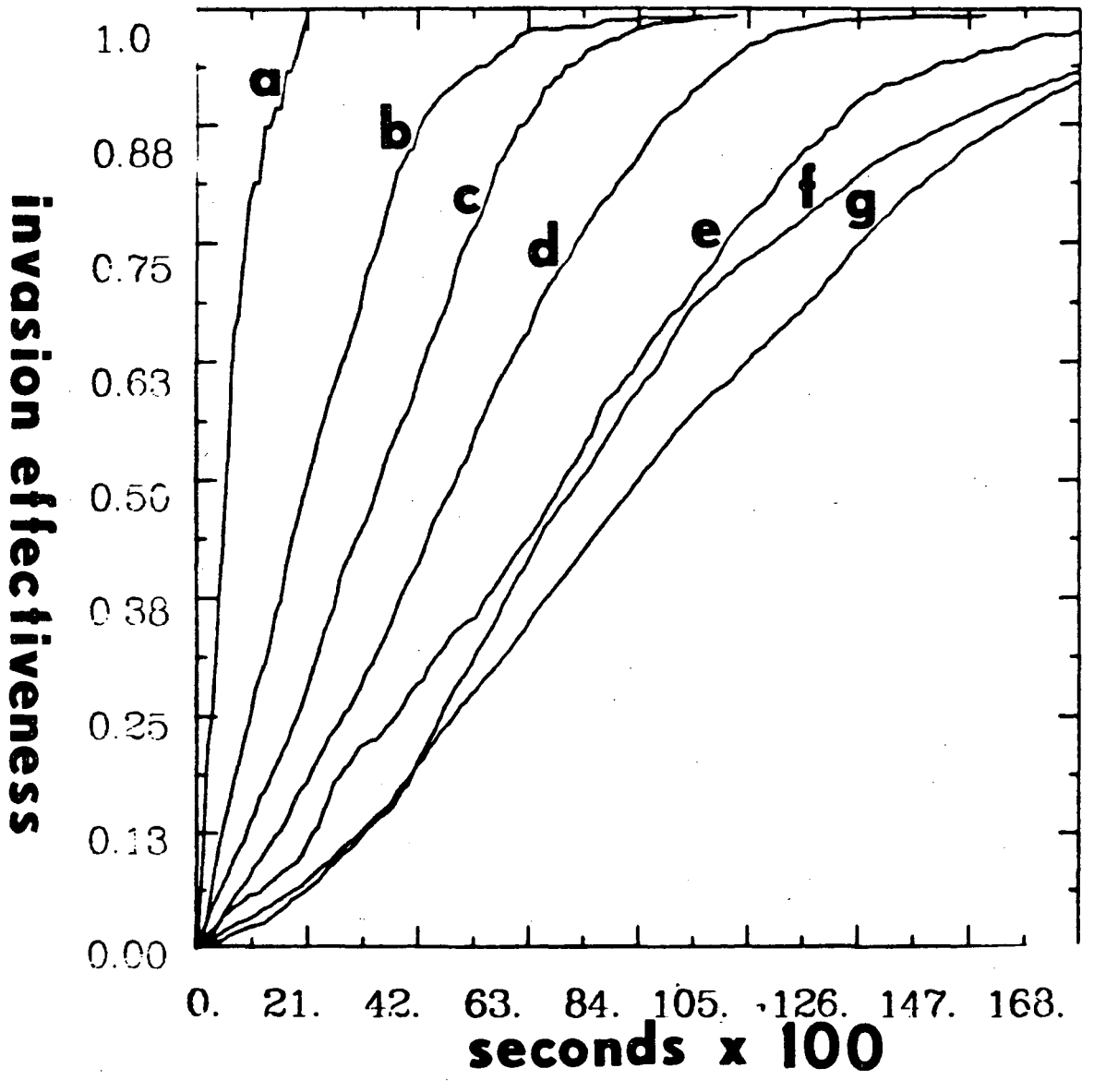
1.0
0.88
0.75
0.63
0.50
0.38
0.25
0.13
0.00
invasion effectiveness
a
b
c
d
e
f
g
0. 21. 42. 63. 84. 105. 126. 147. 168.
seconds x 100

FIGURE 5

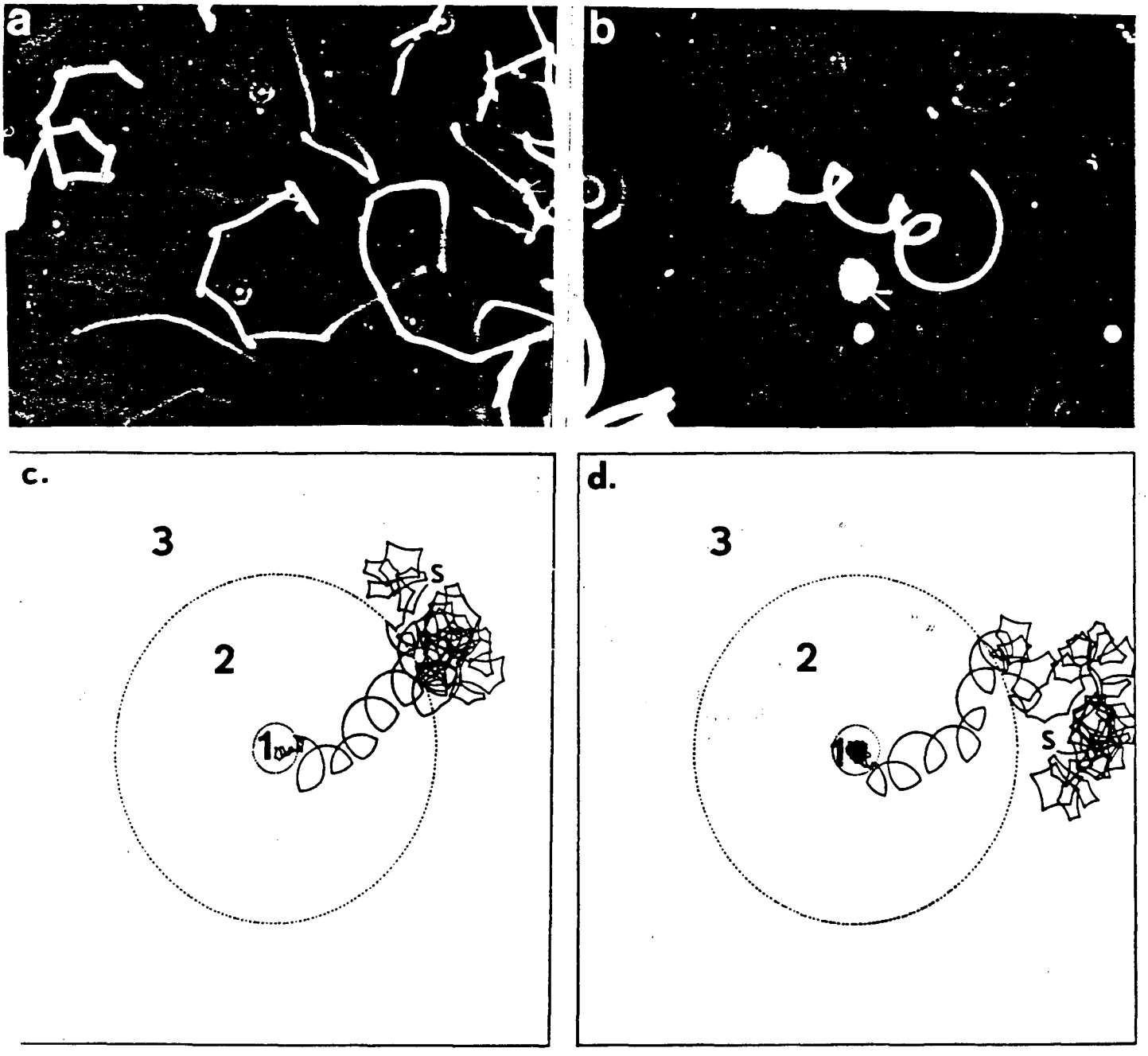

FIGURE 6

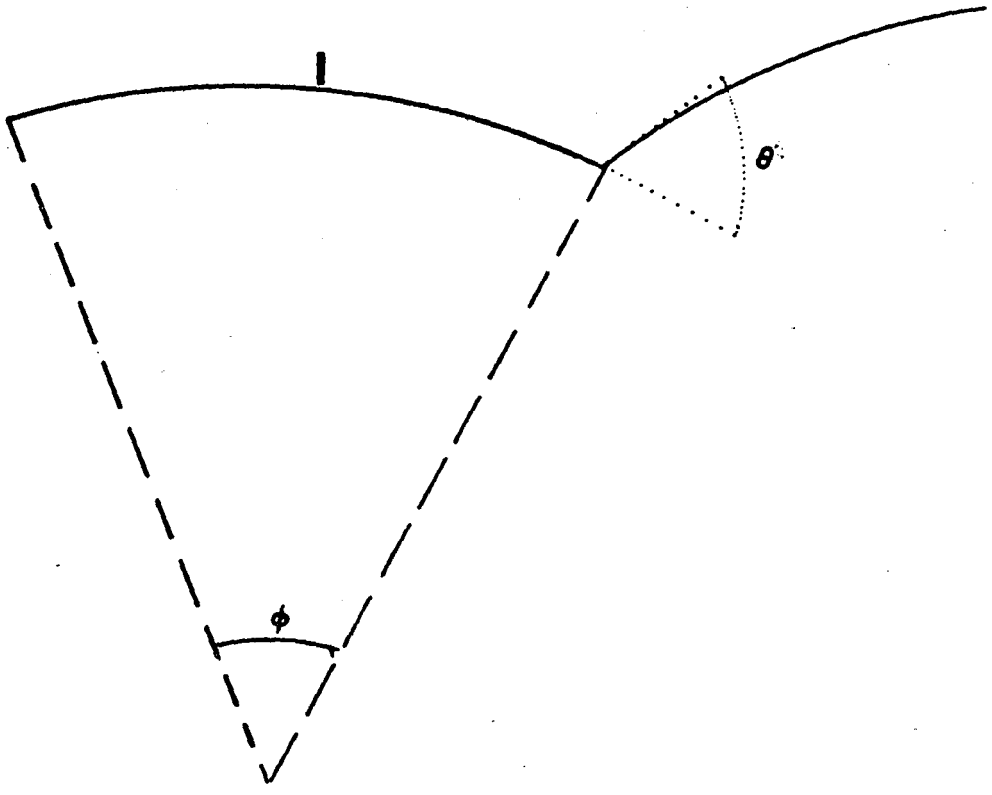

TECHNICAL INFORMATION DEPARTMENT
LAWRENCE BERKELEY LABORATORY
UNIVERSITY OF CALIFORNIA
BERKELEY, CALIFORNIA 94720